2. Antigenic determinants in the GH loop of FMDV C_1-Barcelona

2.0 Introduction

On previous genomic studies of FMDV field isolates, a natural variant, C_1-Barcelona (or C-S30), was characterised as containing four mutations in the GH loop (Ala138→Thr, Ala140→Thr, Leu147→Val and Thr149→Ala) relative to the reference strain C-S8c1 (Table 2.1). Analyses of this four-point mutant by immuno-enzymatic assays showed that it was fully recognised by site A-directed mAbs such as 4C4. Further, this behaviour was confirmed in antigenicity studies of peptide – keyhole limpet hemocyanin (KLH) conjugates reproducing the four relevant mutations[1-7].
The fact that one of the mutations, Leu147→Val, was found to be detrimental for antibody and cell recognition of site A peptides, makes the GH loop of FMDV C-S30 an interesting example to learn more about antigen-antibody recognition mechanisms in FMDV.
The second objective of the present work was, therefore, the synthesis and analysis of peptides mimicking not only the GH loop of the C-S30 strain but also all possible partial mutants of this natural isolate.

2.1 Peptides mimicking the GH loop of FMDV C_1-Barcelona and the corresponding partial mutants

A set of fifteen pentadecapeptides was synthesised, corresponding to all possible combinations of the four mutations found in antigenic site A of C_1-Barcelona (C-S30), taking peptide A15 (GH loop of FMDV C-S8c1) as the reference sequence (Table 2.1).
These peptides were synthesised by machine-assisted parallel solid-phase peptide synthesis, using standard Fmoc/^{t}Bu protocols [8-10] as shown in Fig. 2.1 and described in more detail in section 4.2 (Materials & Methods). Crude peptides were obtained following cleavage from the resin and submitted to further purification (Fig. 2.2) by medium-pressure liquid chromatography (MPLC). Purified products were all satisfactorily identified (MALDI-TOF MS, AAA) as the target peptides, with global yields of *ca.* 50% (Table 2.2). Peptides were lyophilised and stored at – 20 °C prior to their utilisation in subsequent studies.

Table 2.1 Pentadecapeptides reproducing all possible combinations of the mutations found in the GH loop of FMDV C_1-Barcelona (C-S30).

Name	***Sequence***	***Mutants***
A15	**YTASARGDLAHLTTT**	***GH loop of FMDV C-S8c1***
A15(138T)	--T----------	
A15(140T)	----T----------	One-point
A15(147V)	----------V---	
A15(149A)	----------A-	
A15(138T,140T)	--T-T----------	
A15(138T,147V)	--T--------V---	Two-point
A15(138T,149A)	--T----------A-	
A15(140T,147V)	----T------V---	
A15(140T,149A)[a]	----T--------A-	***GH loop of FMDV C_1-Brescia***
A15(147V,149A)	----------V-A-	Two-point
A15(138T,140T,147V)	--T-T------V---	
A15(138T,140T,149A)	--T-T--------A-	Three-point
A15(138T,147V,149A)	--T--------V-A-	
A15(140T,147V,149A)	----T------V-A-	
A15(138T,140T,147V,149A)[b]	--T-T------V-A-	***GH loop of FMDV C-S30***

[a] termed A15Brescia further on.
[b] termed A15S30 further on.

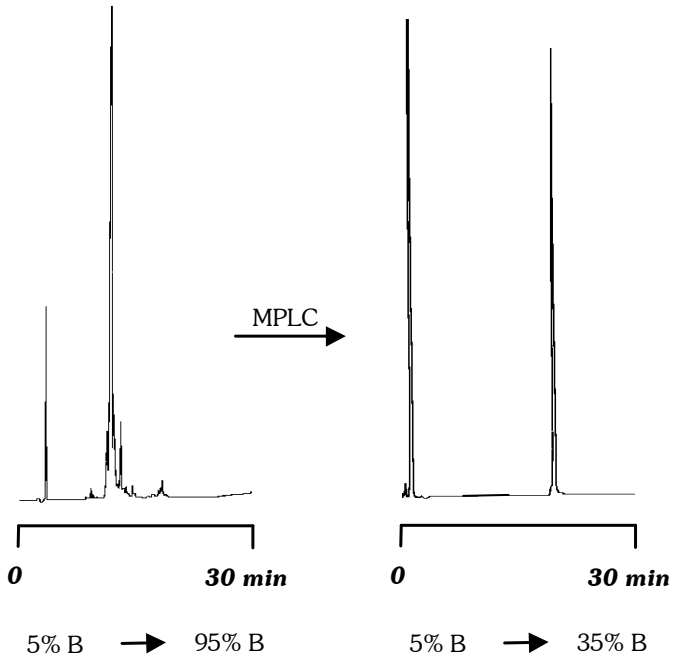

Figure 2. 2 Typical HPLC profiles obtained in the synthesis (left) and purification (right) of the FMDV C-S30 peptides.

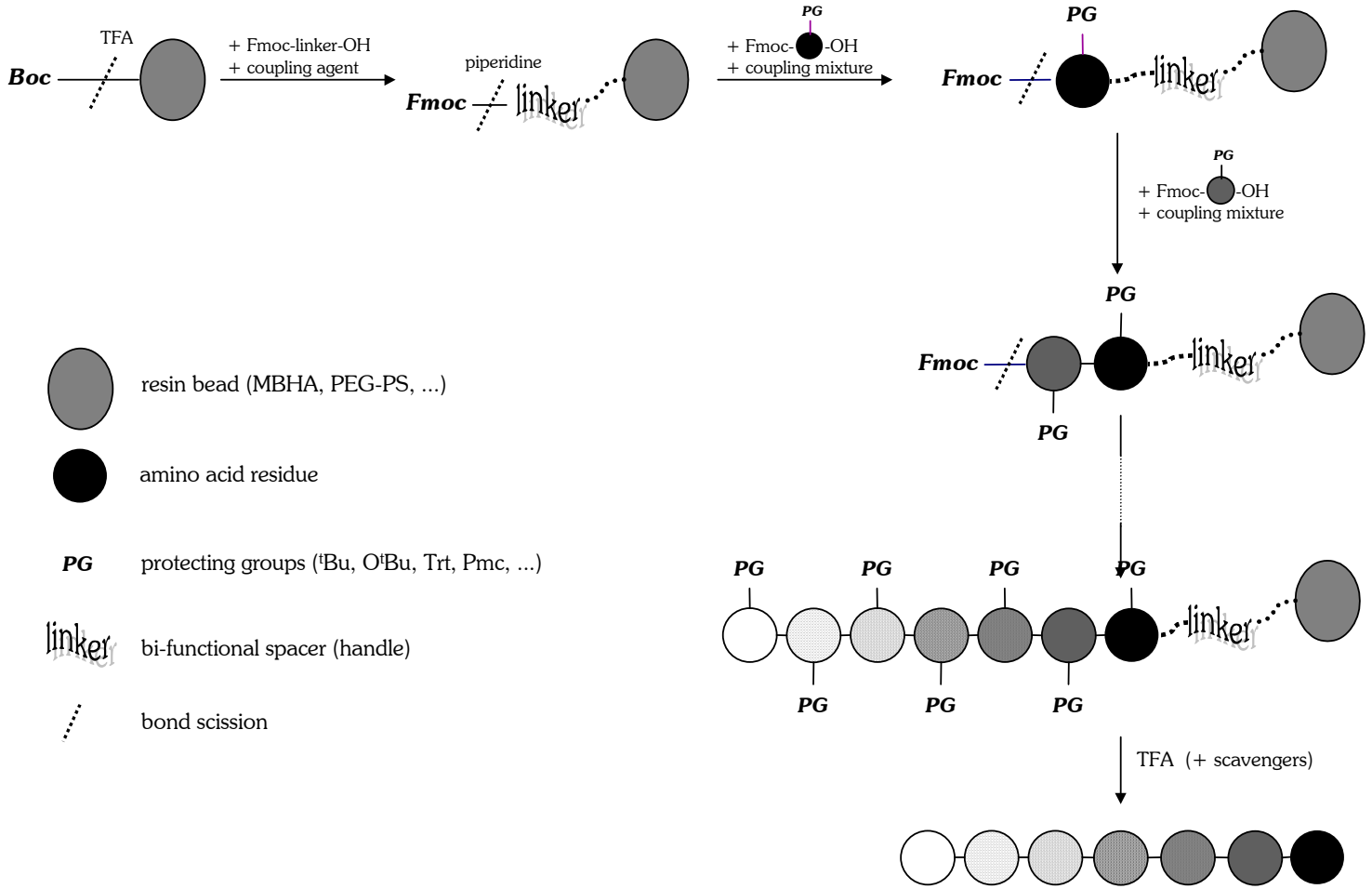

Figure 2. 1 Schematic representation of the general protocol in Fmoc/^{t}Bu solid-phase peptide synthesis (described under Materials & Methods, section 4.2)[8-10].

Table 2.2 Yield, purity (HPLC) and characterisation (MALDI-TOF MS and AAA) of the C-S30 series.

Peptide	***Global yield (%)***	***Purity (% HPLC)***	***MW found***	***MW expected***	***Amino acid analysis (AAA)***
A15(138T)	52	90	1607.2	1607	Asp, 1.12 (1); Ser, 0.94 (1); Gly, 0.98 (1); Ala 2.03 (2); His, 1.08 (1); Arg, 0.85 (1)
A15(140T)	49	81	1607.1	1607	Asp, 0.97 (1); Ser, 0.85 (1); Gly, 1.05 (1); Ala 2.06 (2); His, 1.09 (1); Arg, 0.88 (1)
A15(147V)	43	87	1562.9	1563	Thr, 4.06 (4); Ser, 0.97 (1); Gly, 0.98 (1); Ala 3.06 (3); His, 0.86 (1); Arg, 0.89 (1)
A15(149A)	51	80	1547.1	1547	Asp, 0.92 (1); Ser, 0.80 (1); Gly, 1.03 (1); Ala 4.10 (4); His, 1.06 (1); Arg, 0.99 (1)
A15(138T,140T)	46	85	1636.9	1637	Asp, 1.10 (1); Ser, 0.88 (1); Gly, 1.07 (1); Ala 1.06 (1); Leu, 2.01 (2); His, 0.87 (1)
A15(138T,147V)*	10	76	1592.8	1593	Asp, 0.96 (1); Ser, 1.13 (1); Val, 0.95 (1); Leu, 1.15 (1); His, 0.95 (1); Arg 1.01 (1)
A15(138T,149A)	50	96	1576.9	1577	Asp, 0.94 (1); Ser, 0.91 (1); Gly, 1.06 (1); Leu, 2.04 (2); His, 0.97 (1); Arg, 0.91 (1)
A15(140T,147V)	41	94	1592.7	1593	Asp, 0.90 (1); Ser, 0.87 (1); Gly, 1.07 (1); Ala 2.09 (2); Leu, 1.10 (1); Arg, 0.84 (1)
A15Brescia	36	91	1576.9	1577	Asp, 0.95 (1); Ser, 0.87 (1); Gly, 1.06 (1); Ala 3.06 (3); Leu, 1.99 (2); His, 0.94 (1)
A15(147V,149A)*	21	79	1533.1	1533	Asp, 0.71 (1); Gly, 1.07 (1); Ala 4.04 (4); Val, 0.68 (1); Leu, 1.03 (1); Arg, 0.86 (1)
A15(138T,140T,147V)	48	93	1623.6	1623	Asp, 1.03 (1); Ser, 0.88 (1); Gly, 1.09 (1); Ala 1.08 (1); Leu, 1.08 (1); Arg, 0.84 (1)
A15(138T,140T,149A)	41	91	1607.6	1607	Asp, 0.92 (1); Ser, 0.81 (1); Gly, 1.06 (1); Ala 2.14 (2); Leu, 1.96 (2); His, 0.92 (1)
A15(138T,147V,149A)	52	98	1562.9	1563	Asp, 0.98 (1); Ser, 0.90 (1); Gly, 1.01 (1); Ala 3.06 (3); Leu, 1.04 (1); Arg, 1.01 (1)
A15(140T,147V,149A)		98	1562.9	1563	Asp, 1.02 (1); Ser, 0.86 (1); Gly, 1.03 (1); Ala 3.04 (1); Leu, 1.05 (1); Arg, 0.82 (1)
A15S30	59	99	1592.7	1593	Asp, 1.10 (1); Ser, 0.88 (1); Gly, 1.07 (1); Ala 1.06 (1); Leu, 2.01 (2); His, 0.87 (1)

* These syntheses were carried out under sub-optimal conditions due to instrumental malfunction.
Relative amino acid ratios found by AAA are followed by the expected value in parenthesis.

2.2 SPR study of the C-S30 peptides

Having found suitable experimental conditions for the SPR kinetic study of interactions between FMDV peptides in solution and immobilised anti-FMDV antibodies, as described in chapter 1, SPR was again chosen for the characterisation of the C-S30 peptides. This would allow the detailed study of the effects caused by the stepwise introduction of the four mutations found in the GH loop of FMDV C-S30 and provide a possible explanation for the peculiar behaviour of this virus isolate.

The C-S30 pentadecapeptides were, therefore, screened by SPR against three anti-site A monoclonal antibodies, SD6, 4C4 and 3E5[A].

The three mAbs were immobilised on CM5 sensor chips following standard protocols, with final immobilisation densities of about 1600 RU. Sensorgrams were obtained and analysed as previously described (chapter 1) and all measurable interactions fitted to the 1:1 langmuirian interaction kinetic model (often considering baseline drift). Whenever interactions could not be reliably measured, sensorgrams had a square-wave like shape, either due to bulk refractive index response or to extremely fast on/off rates. Although the monitored on/off rates were generally high, and consequently liable to be under mass-transport effects, the quantitative data obtained appeared to be self-consistent and were thus considered reliable. Discussion of the results is presented in the following sections.

2.2.1 One-point mutants

As observed in previous studies by competition ELISA, SPR analysis showed that substitutions Ala140→Thr and Thr149→Ala were well tolerated by the three mAbs. This was to be expected, since both replacements are present in field isolate C_1-Brescia, previously shown to be recognised by these mAbs[4].

Mutations Ala138→Thr and Leu147→Val affected antibody recognition to different extents: mAb SD6 was more sensitive to Ala138→Thr than to Leu147→Val, quite the opposite to mAb 4C4, which tolerated the first replacement much better than the second one. Similar effects were observed for mAb 3E5. These results are consistent with recent crystallographic studies, where it was found that Ala138 has a higher percentage of residue contact with mAb SD6 than with mAb 4C4[14].

Peptide affinities to each mAb are mainly reflected in the different dissociation rate constants observed for the corresponding peptide-mAb complexes (Table 2.3), as further illustrated in Fig. 2.3.

[A] this anti-site A mAb was raised against FMDV strain C_1-Brescia. Ascitic fluid of mAb 3E5 was kindly supplied by Dr. Emiliana Brocchi (IZSLE – Brescia, Italy).

Table 2.3 Kinetic SPR analysis of the interactions between FMDV C-S30 peptides and mAbs SD6, 4C4 and 3E5.

mAb	***SD6***			***4C4***			***3E5***		
Peptide	$k_a/M^{-1}s^{-1}$	k_d/s^{-1}	K_A/M^{-1}	$k_a/M^{-1}s^{-1}$	k_d/s^{-1}	K_A/M^{-1}	$k_a/M^{-1}s^{-1}$	k_d/s^{-1}	K_A/M^{-1}
A15	7.3×10^{4}	1.4×10^{-3}	$\mathbf{5.4\times10^{7}}$	3.8×10^{5}	1.9×10^{-3}	$\mathbf{1.9\times10^{8}}$	1.6×10^{5}	1.6×10^{-3}	$\mathbf{9.4\times10^{7}}$
A15(138T)	1.0×10^{5}	1.5×10^{-2}	$\mathbf{6.5\times10^{6}}$	2.5×10^{5}	5.9×10^{-3}	$\mathbf{4.2\times10^{7}}$	1.1×10^{5}	8.5×10^{-3}	$\mathbf{1.3\times10^{7}}$
A15(140T)	1.4×10^{5}	3.0×10^{-3}	$\mathbf{4.7\times10^{7}}$	6.0×10^{5}	2.6×10^{-3}	$\mathbf{2.3\times10^{8}}$	2.6×10^{5}	1.5×10^{-3}	$\mathbf{1.8\times10^{8}}$
A15(147V)	1.1×10^{5}	1.0×10^{-2}	$\mathbf{1.0\times10^{7}}$	9.5×10^{4}	4.4×10^{-2}	$\mathbf{2.2\times10^{6}}$	3.3×10^{5}	5.0×10^{-2}	$\mathbf{6.6\times10^{6}}$
A15(149A)	1.2×10^{5}	2.2×10^{-3}	$\mathbf{5.5\times10^{7}}$	6.4×10^{5}	3.1×10^{-3}	$\mathbf{2.1\times10^{8}}$	4.8×10^{5}	1.5×10^{-3}	$\mathbf{3.2\times10^{8}}$
A15(138T,140T)	1.6×10^{5}	1.5×10^{-2}	$\mathbf{1.1\times10^{7}}$	2.6×10^{5}	8.2×10^{-3}	$\mathbf{3.1\times10^{7}}$	2.4×10^{5}	8.4×10^{-3}	$\mathbf{2.9\times10^{7}}$
A15(138T,147V)	3.8×10^{4}	4.2×10^{-2}	$\mathbf{9.1\times10^{5}}$	2.4×10^{5}	4.2×10^{-2}	$\mathbf{5.7\times10^{6}}$	2.6×10^{5}	4.2×10^{-2}	$\mathbf{6.3\times10^{6}}$
A15(138T,149A)	1.2×10^{5}	1.7×10^{-2}	$\mathbf{7.0\times10^{6}}$	2.5×10^{5}	3.2×10^{-3}	$\mathbf{7.6\times10^{7}}$	3.2×10^{5}	8.3×10^{-3}	$\mathbf{3.9\times10^{7}}$
A15(140T,147V)	7.8×10^{4}	1.3×10^{-2}	$\mathbf{6.1\times10^{6}}$	2.4×10^{5}	6.5×10^{-2}	$\mathbf{3.7\times10^{6}}$	3.8×10^{5}	4.8×10^{-2}	$\mathbf{8.0\times10^{6}}$
A15Brescia	9.0×10^{4}	8.0×10^{-3}	$\mathbf{1.2\times10^{7}}$	2.6×10^{5}	1.6×10^{-3}	$\mathbf{1.6\times10^{8}}$	4.4×10^{5}	4.2×10^{-3}	$\mathbf{1.0\times10^{8}}$
A15(147V,149A)	1.0×10^{5}	1.7×10^{-2}	$\mathbf{6.0\times10^{6}}$	2.1×10^{5}	4.4×10^{-2}	$\mathbf{4.7\times10^{6}}$	4.8×10^{5}	3.7×10^{-2}	$\mathbf{1.3\times10^{7}}$
A15(138T,140T,147V)		ni		3.4×10^{5}	1.6×10^{-1}	$\mathbf{2.1\times10^{6}}$		ni	
A15(138T,140T,149A)	2.2×10^{5}	2.2×10^{-2}	$\mathbf{9.7\times10^{6}}$	2.1×10^{5}	9.6×10^{-3}	$\mathbf{2.2\times10^{7}}$	3.4×10^{5}	1.4×10^{-2}	$\mathbf{2.5\times10^{7}}$
A15(138T,147V,149A)		ni		3.1×10^{5}	$5.2\times10^{-2*}$	$\mathbf{6.0\times10^{6}}$	3.6×10^{5}	4.1×10^{-2}	$\mathbf{8.9\times10^{6}}$
A15(140T,147V,149A)	1.7×10^{5}	1.8×10^{-2}	$\mathbf{9.1\times10^{6}}$	4.4×10^{5}	$7.2\times10^{-2*}$	$\mathbf{6.1\times10^{6}}$	5.9×10^{5}	$5.2\times10^{-2*}$	$\mathbf{1.1\times10^{7}}$
A15S30	3.8×10^{4}	$8.8\times10^{-2*}$	$\mathbf{4.3\times10^{5}}$	2.2×10^{5}	$1.2\times10^{-1*}$	$\mathbf{2.0\times10^{6}}$	3.2×10^{5}	$7.2\times10^{-2*}$	$\mathbf{4.5\times10^{6}}$

* Although resulting from apparently reliable data fits, k_d values equal or higher than 5×10^{-2} should be regarded with some caution, since this value is considered the limit of reliable SPR measurement of rate constants; "ni" denotes interactions which could not be reliably measured.

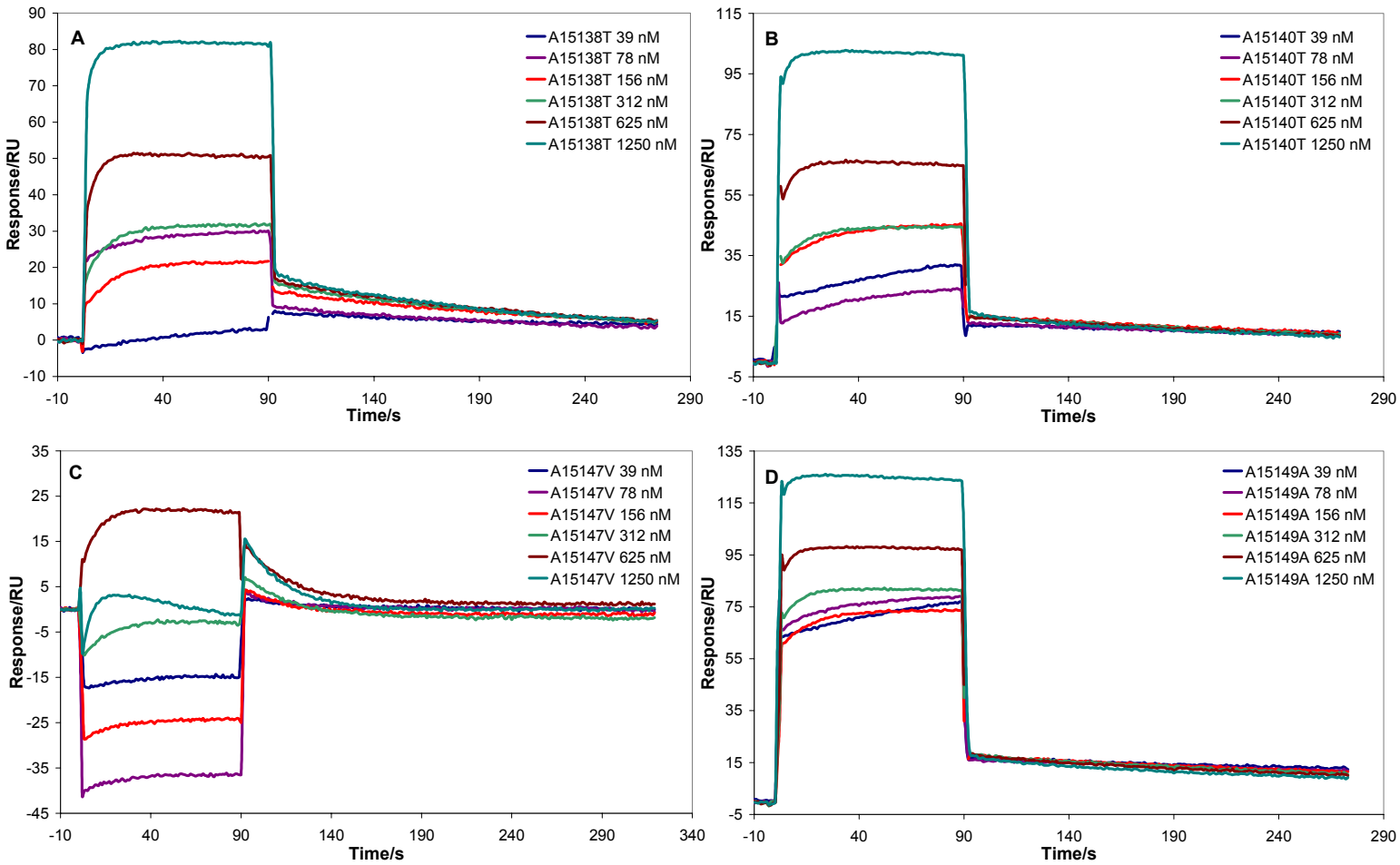

Figure 2. 3 Sensorgrams obtained in the SPR kinetic analysis of the interactions between immobilised mAb 4C4 and: ***A.*** peptide A15(138T); ***B.*** peptide A15(140T); ***C.*** peptide A15(147V) and ***D.*** peptide A15(149A). This figure illustrates the differences observed in the dissociation rate constants for each mAb-peptide interaction.

2.2.2 Two- and three-point mutants

Analysis of data in Table 2.3 immediately suggests that two- and three-point combinations of the amino acid replacements are additive. Indeed, antigenicities of the two- and three-point mutant peptides towards the three mAbs employed reflect the combined effects of the single-point mutations present in each particular sequence. This effect is further confirmed when comparing the experimental relative affinities [$K_{Arel}=K_A(peptide)/K_A(A15)$] with the calculated relative affinities assuming additive effects in the combination of single-point mutations [expected $K_{Arel} = K_{Arel}$(single-point mutant 1) $\times$ K_{Arel}(single-point mutant 2) $\times$ ... $\times$ K_A(peptide A15)], as illustrated in Fig. 2.4. Peptide A15Brescia (with replacements A140→T and T149→A) was the most antigenic within the group of multiple-point mutants (Table 2.4). Interestingly, for this peptide the correlation between experimental and calculated relative affinities was poorer than for all the other mutants, suggesting a compensatory effect (*i.e.*, lack of additivity) between both replacements. On the other hand, peptides containing the L147→V substitution were the poorest antigens, particularly when the A138→T replacement was also present. Further, affinities were again almost exclusively determined by the dissociation rates of peptide – mAb complexes (compare data within each mAb set in Table 2.3).

2.2.3 Four-point mutant: peptide A15S30

The most striking result obtained in this SPR screening of FMDV peptides was the low affinity observed for peptide A15S30 (reproducing the GH loop of FMDV C-S30) towards all three mAbs assayed. Although such low antigenicity was totally in agreement with the additive effects observed when combining the different individual substitutions in the partial mutants (Fig. 2.4), previous studies with FMDV C-S30 had shown that this natural isolate was neutralised by mAb 4C4[15] and, further, that the KLH conjugate of a 21-mer peptide reproducing the C-S30 loop had been fully recognised by the same mAb in immuno-enzymatic assays[6,7].

Despite the fact that SPR data was apparently self-consistent and reliable, we decided to perform a qualitative comparison between the SPR affinities of peptides A15, A15Brescia and A15S30 using a reverse SPR configuration: peptide immobilisation and mAb as soluble analyte, as described under Materials & Methods (section 4.3.1). Even though this configuration was not optimised (to avoid artefacts such as diffusion controlled kinetics or ligand heterogeneity[11]), the performance of all assays under identical conditions and the high molecular weight of the mAb analytes would provide both high SPR responses and a reliable qualitative comparison between the three peptide antigens. As shown in Table 2.4 and Fig. 2.5, this assay further confirmed the above SPR data: although rate constants for peptide – mAb interaction depended on the analysis format (consistently lower in the format with mAb as analyte), thermodynamic affinities were virtually the same and the antigenicity ranking was identical to the one derived from the first SPR analysis of these peptides. Since these

SPR results did not agree with the neutralisation and immuno-enzymatic data discussed above, a competition ELISA screening of all C-S30 peptides synthesised towards the three mAbs was performed, as described in section 2.3.

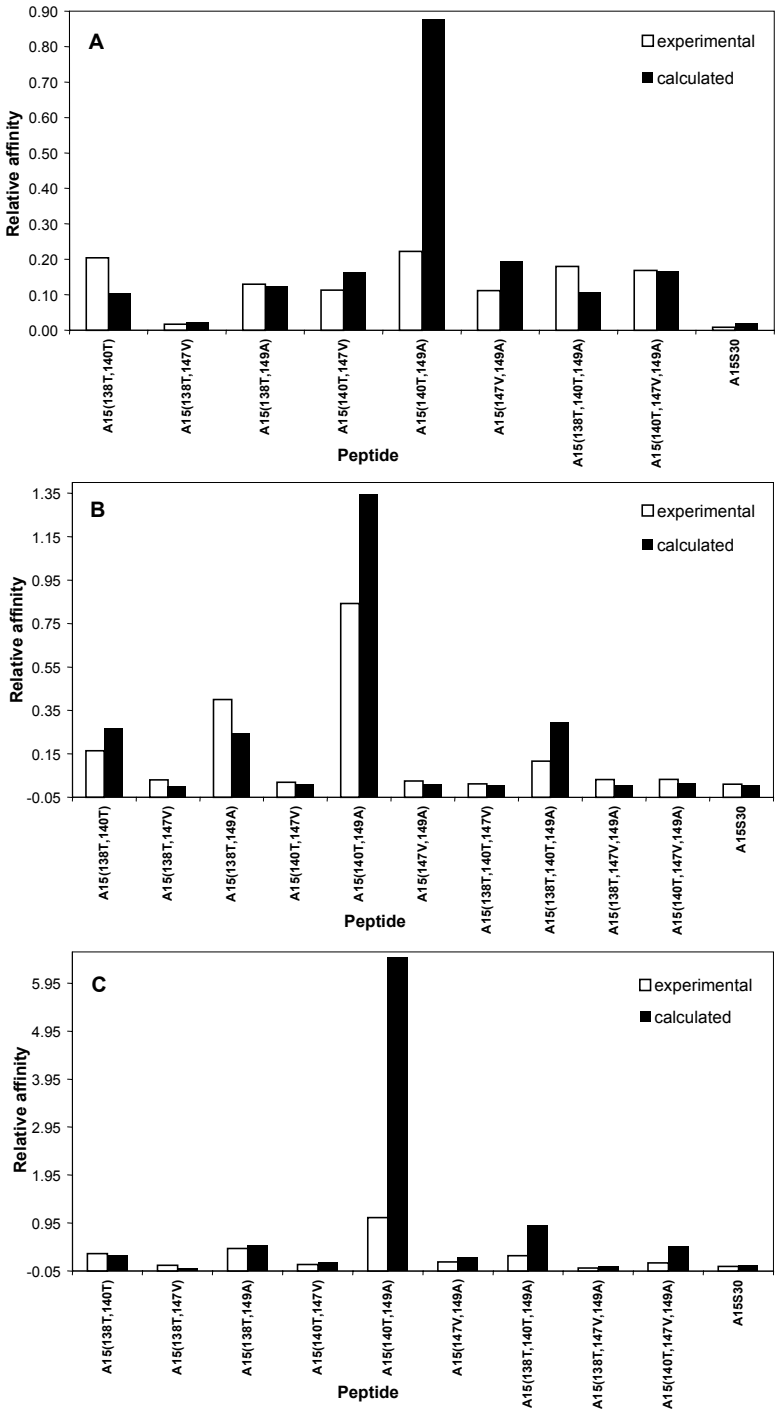

Figure 2. 4 Experimental and calculated affinities of A15 mutant peptides towards mAbs SD6 (A), 4C4 (B) and 3E5 (C). Calculated values have been determined assuming additive effects of the amino acid replacements (see text).

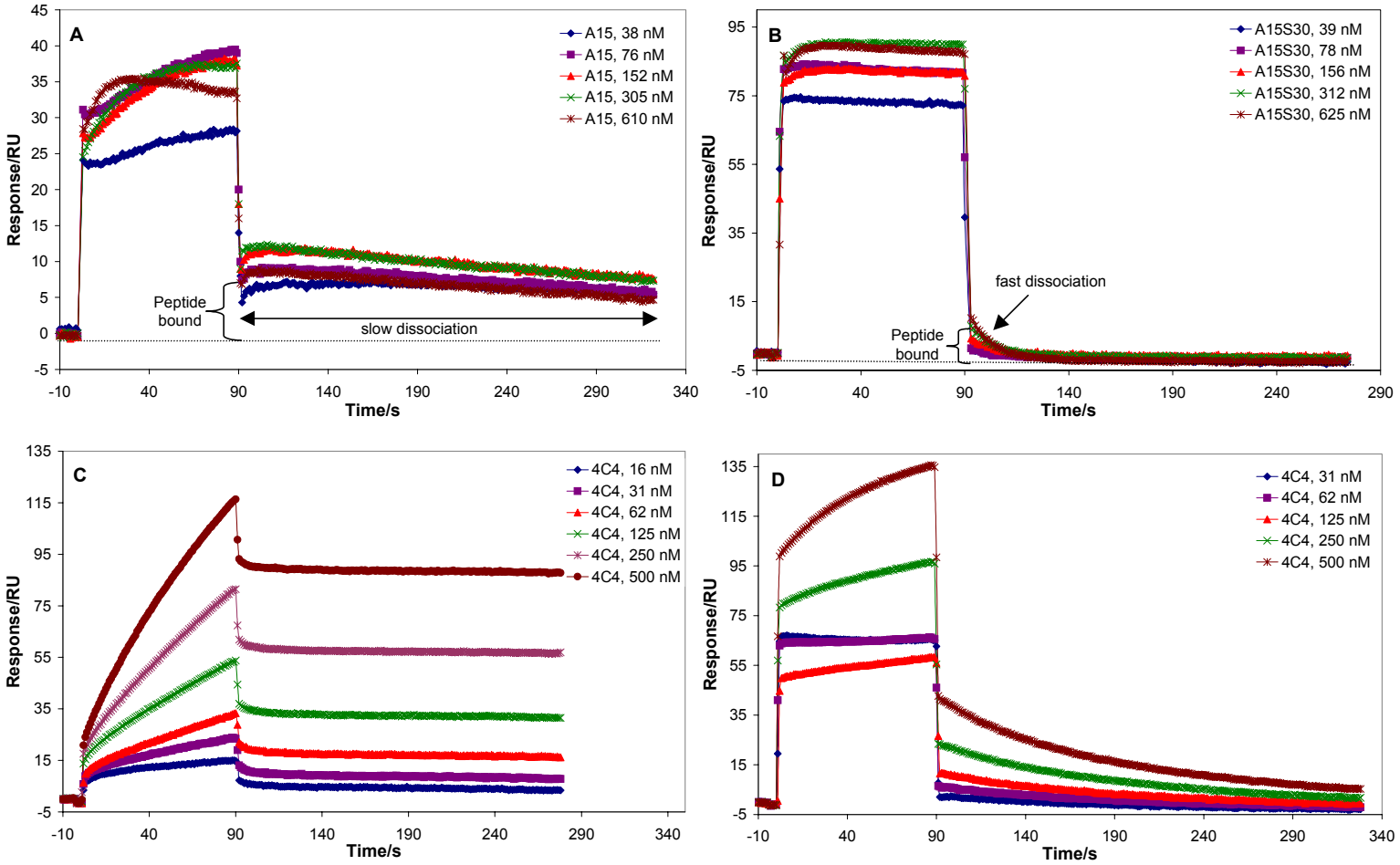

Figure 2. 5 Sensorgrams from the SPR direct analysis of the interactions between peptides A15 and A15S30 with mAb 4C4: ***A.*** immobilised mAb *vs.* A15; ***B.*** immobilised mAb *vs.* A15S30; ***C.*** immobilised A15 *vs.* 4C4; ***D.*** immobilised A15S30 *vs.* 4C4.

Table 2.4 Kinetic analyses using peptides immobilised on the chip.

mAb	***Peptide***	$k_a/M^{-1}s^{-1}$	k_d/s^{-1}	K_A/M^{-1}
SD6	A15	1.2×10^{4}	2.5×10^{-4}	5.0×10^{7}
	A15Brescia*	1.8×10^{4}	-	-
	A15S30	2.9×10^{3}	1.8×10^{-2}	1.6×10^{5}
4C4	A15	2.3×10^{4}	2.2×10^{-4}	1.1×10^{8}
	A15Brescia*	1.8×10^{4}	-	-
	A15S30	2.5×10^{4}	1.1×10^{-2}	2.3×10^{6}
3E5	A15	1.2×10^{5}	7.3×10^{-4}	1.7×10^{8}
	A15Brescia*	1.7×10^{4}	-	-
	A15S30	3.5×10^{4}	1.1×10^{-2}	3.2×10^{6}

* k_d too small to be reliably measured; k_a determined from the linear dependence of k_s (global rate constant=$k_a\times C+k_d$) on analyte concentration.

2.2.4 A possible significance for kinetic rate constants in antigen-antibody interactions

As already mentioned, a consistent observation in the present study was that peptide – antibody affinities seem mainly determined by the dissociation rate constant, k_d (Table 2.3). Hence, for a given family of peptide analogues, a higher or lower antigenicity towards a given mAb would exclusively depend on the half-life ($t_{1/2}$) of the complex. Thus, all analogues would be similarly capable of approaching the mAb paratope but, once there, their different ability to establish complex-stabilising interactions would dictate the life-time of the complex and, consequently, peptide – antibody affinity (K_D). If this interpretation was true, the association rate constant (k_a) would be sequence-independent and only determined by the global fitness of the antibody paratope ($K_D \propto k_d \Rightarrow k_a$ = constant) to a series of analogue antigens. Indeed, a closer look at the kinetic data of the SPR screening of 15-mer peptides (Table 2. 3) suggests that this might be the case. Plotting affinities (K_D) against dissociation rate constants (k_d) gives for each mAb a set of points for which a correlation line with a satisfactory r^2 coefficient (>0.9) can be derived (Fig. 2.6). The slopes of these three lines correlate well with the reciprocal of the average association rates of the interactions among each mAb and the entire set of peptide antigens. Thus, slope of SD6 correlation line is 1×10^{-5} *vs.* 1/average $k_a = 9.0\times10^{-6}$. Similarly, for 4C4, slope = 4×10^{-6} *vs.* 1/average $k_a = 3.1\times10^{-6}$; and for 3E5, slope = 3×10^{-6} *vs.* 1/average $k_a = 3.4\times10^{-6}$.

Of course, these correlations would only apply to relatively similar sets of analogue antigens; more drastic changes in antigen size, folding or amino acid composition would certainly be expected to lead to substantial changes in both dissociation and association rate constants.

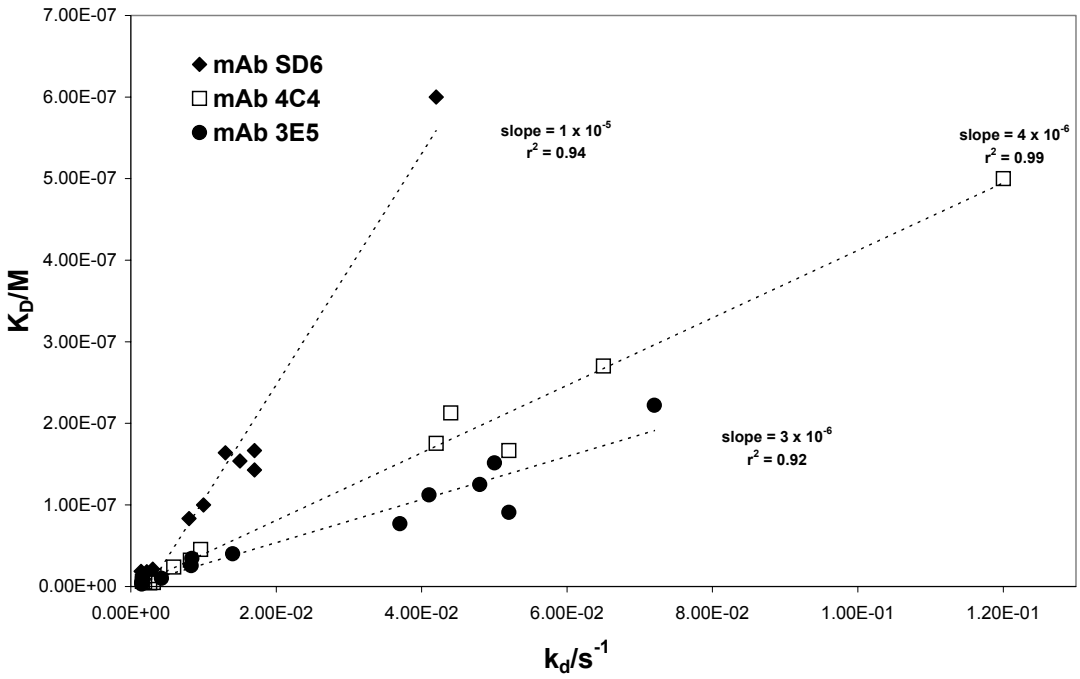

Figure 2. 6 Correlation between thermodynamic affinity (K_D) and kinetic dissociation constant (k_d) for the SPR-measured interactions between C-S30 peptides and three anti-FMDV mAbs SD6, 4C4 and 3E5.

2.3 Competition ELISA analysis of the C-S30 pentadecapeptides

As already mentioned, in view of the surprisingly low affinity shown by the A15S30-4C4 complex on SPR, a competition ELISA (Fig. 2.7) screening of all the C-S30 pentadecapeptides was performed[16,17]. For this purpose, 96-well plates were coated with an FMDV C-S8c1 reference antigen, the KLH conjugate of peptide A21 (corresponding to a 6-residue extension at the C-terminus of peptide A15):

YTASARGDLAHLTTTHARHLP *A21*

Equilibrium mixtures of the competitor at different concentrations with constant concentrations of the mAb were incubated and the amount of mAb which bound to antigen was measured. Plotting the variation of plate-bound mAb with competitor peptide concentration gave inhibition curves such as those in Fig. 2.8, thus providing an evaluation of competitor peptide antigenicity. This antigenicity was expressed in terms of relative IC_{50} (concentration of competitor producing 50% inhibition), where relative means normalised with respect to the IC_{50} of peptide A15. As can be seen from Figs. 2.8 and 2.9, data derived from competition ELISA were in good agreement with previous SPR results, in the sense that the poorest antigens in SPR were also the worse competitors in ELISA. These results demonstrate that the low A15S30-4C4 affinity previously obtained did not come from eventual artefacts in SPR analysis.

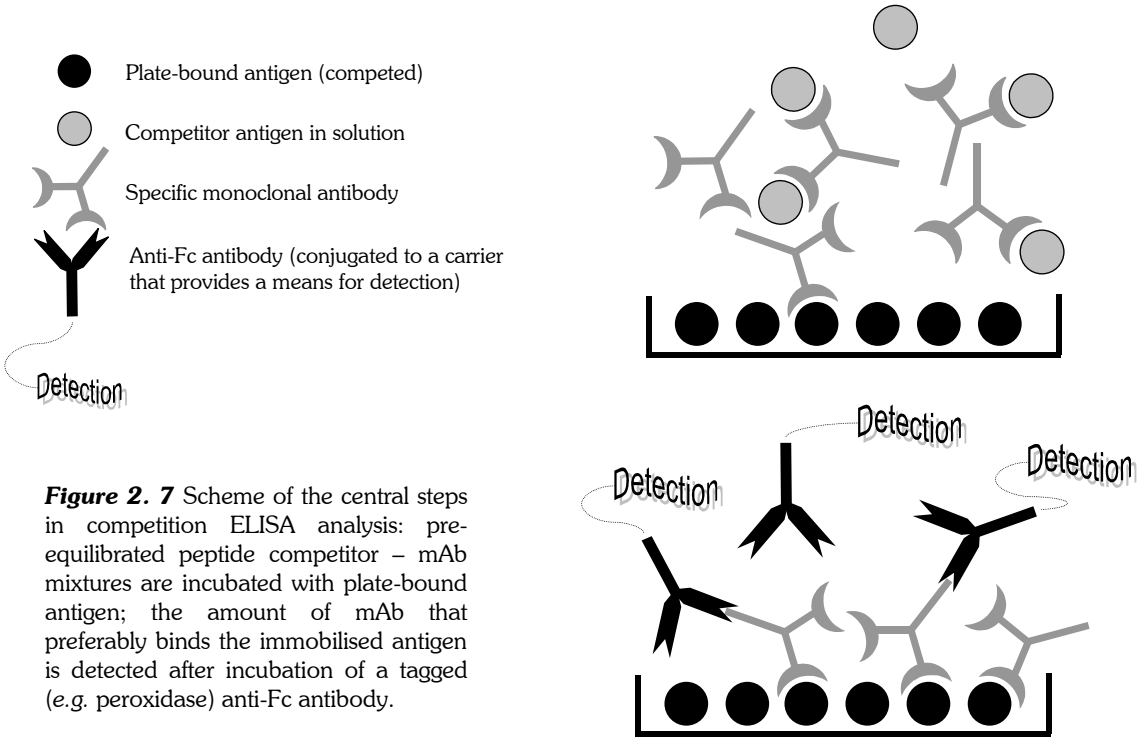

Figure 2. 7 Scheme of the central steps in competition ELISA analysis: pre-equilibrated peptide competitor – mAb mixtures are incubated with plate-bound antigen; the amount of mAb that preferably binds the immobilised antigen is detected after incubation of a tagged (*e.g.* peroxidase) anti-Fc antibody.

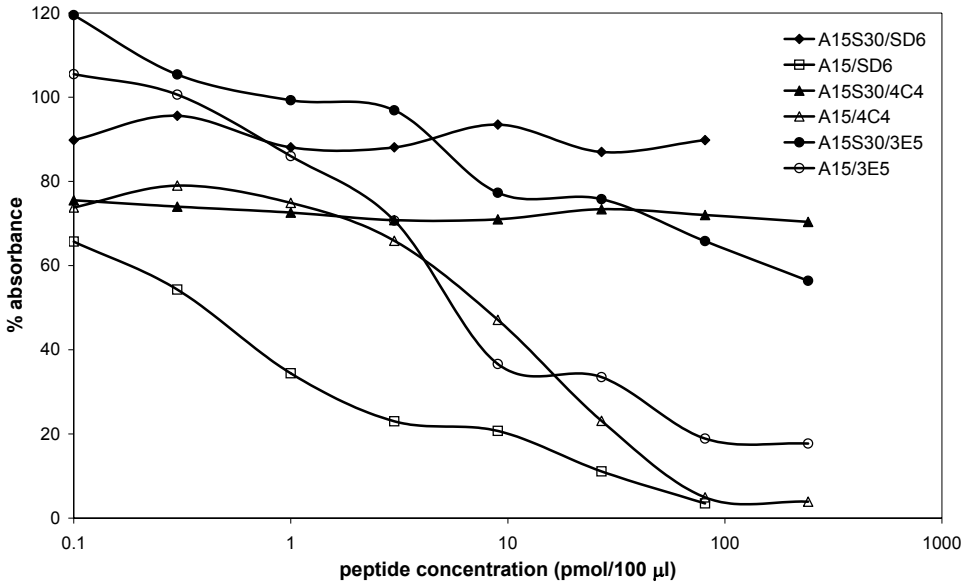

Figure 2. 8 Competition between plate-bound A21 – KLH and pentadecapeptides A15 and A15S30 for anti-site A mAbs.

% Percentage of the maximal absorbance measured for mAb incubated with plate-bound antigen in the absence of peptide competitor; all absorbances were corrected by subtraction of mean absorbance obtained for negative controls.

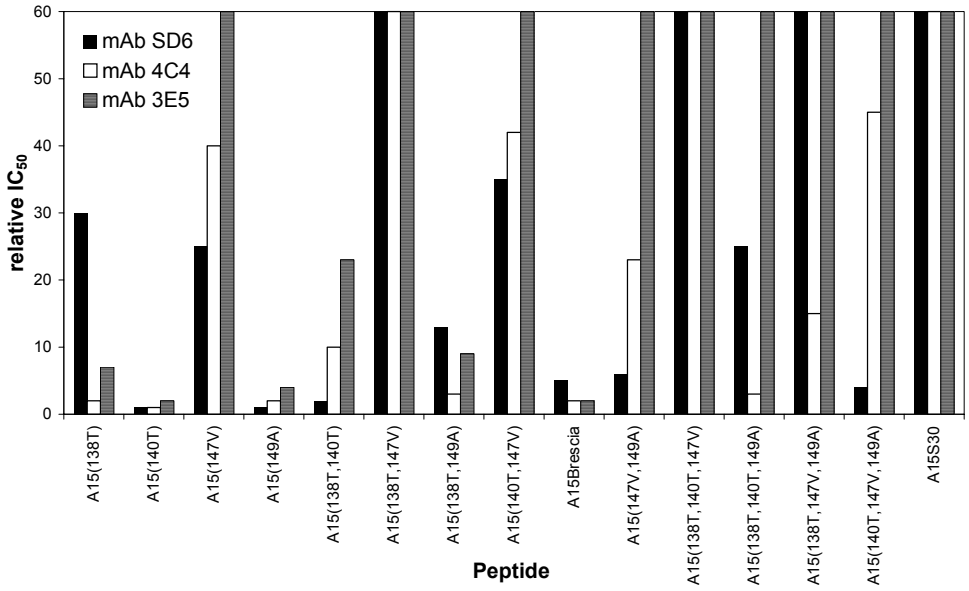

Figure 2. 9 Screening of the C-S30 pentadecapeptides by competition ELISA.

IC_{50} values were normalised to IC_{50} of peptide A15; IC_{50} higher than the maximum competitor concentration are truncated at 60.

2.4 Size effects in the antigenicity of C-S30 peptides

The observation of a low antigenicity for peptide A15S30 in solution, and the confirmation that it was not artefactual (*e.g.* peptide instability or aggregation) prompted us to investigate if the discrepancies between our measurements and previous immunoenzymatic results[1-7] could be due to the small size of our peptides. Therefore, two additional 21-mer versions of antigenic site A in FMDV strains C-S8c1 (peptide A21) and C-S30 (peptide A21S30) were synthesised and analysed by SPR and competition ELISA.

YTASARGDLAHLTTTHARHLP *A21*

YT**T**S**T**RGDLAH**V**T**A**THARHLP *A21S30*

2.4.1 Synthesis of 21-mer peptides reproducing antigenic site A from FMDV strains C-S8c1 and C-S30

Synthetic procedures and results of the synthesis and purification of these 21-mer peptides were identical to those described in section 2.1, employing either manual or machine-assisted Fmoc/^{t}Bu solid-phase peptide synthesis (see Materials & Methods, section 4.2). The results are summarised in Table 2.5.

Table 2.5 Synthesis data of A21 and A21S30.

Peptide	*Global yield (%)*	*Purity (% HPLC)*	*MW found*	*MW expected*	*AAA**
A21	37	94	2302.6	2303	Asp, 0.97 (1); Gly, 1.06 (1); Ala, 3.89 (4); Leu, 3.19 (3); His, 2.87 (3); Pro, 1.12 (1)
A21S30	31	98	2287.8	2288	Asp, 0.93 (1); Gly, 0.91 (1); Ala, 3.12 (3); Leu, 2.17 (2); His, 3.02 (3); Pro, 1.08 (1)

* Relative amino acid ratios given by AAA are followed by the theoretical values in parenthesis.

2.4.2 Antigenic analyses of A21 and A21S30 by SPR and competition ELISA

Peptides A21 and A21S30 were studied by SPR using peptide as either analyte or immobilised ligand. As already explained in section 2.2.3, SPR analyses using immobilised peptide were not fully optimised for artefacts such as ligand heterogeneity or mass-transport limitations. This is reflected in the lower kinetic constants measured when using mAb as analyte. Nevertheless, one of our major goals in the present work has been the application of SPR analysis to screen small antigenic peptides as analytes and all experiments in the reverse format should be regarded as merely comparative.

SPR data of the interactions between peptide A21S30 and the anti-GH loop mAbs are displayed in Table 2.6. Parallel analyses of peptide A21 were also performed but could not be accurately quantitated due to either insufficient surface regeneration (using mAb immobilised on the chip) or extremely small off-rates (using peptide immobilised on the chip). Only the interaction between immobilised SD6 and A21 could be measured: $k_a=1.3\times10^5$ $M^{-1}s^{-1}$, $k_d=6.1\times10^{-3}$ s^{-1}, $K_A=2.1\times10^7$ M^{-1}. Although this was a serious drawback for an accurate evaluation of the antigenicity of A21, it provided further evidence of the high affinity of the C-S8c1 peptides towards anti-GH loop mAbs. In turn, peptide A21S30 displayed high dissociation rate constants (k_d) as previously observed with the shorter 15-mer peptide A15S30 (Fig. 2.10). A slight increase in affinity could be observed upon addition of further 6 amino amino acid residues to the sequence of the C-S30 GH loop, but such increase was also qualitatively observed for the C-S8c1 sequence, thus maintaining the antigenicity ranking already observed and discussed in previous sections.

Table 2.6 Interactions of anti-site A mAbs with A21S30.

mAb \ ***Peptide A21S30***		***as analyte***	***immobilised on the chip***
SD6	$k_a/M^{-1}s^{-1}$	8.6×10^4	5.4×10^3
	k_d/s^{-1}	2.9×10^{-2}	4.3×10^{-3}
	K_A/M^{-1}	$\mathbf{3.0\times10^6}$	$\mathbf{1.2\times10^6}$
4C4	$k_a/M^{-1}s^{-1}$	2.4×10^5	2.5×10^4
	k_d/s^{-1}	4.3×10^{-2}	3.7×10^{-3}
	K_A/M^{-1}	$\mathbf{5.6\times10^6}$	$\mathbf{6.8\times10^6}$
3E5	$k_a/M^{-1}s^{-1}$	2.8×10^5	5.0×10^4
	k_d/s^{-1}	5.0×10^{-2}	4.8×10^{-3}
	K_A/M^{-1}	$\mathbf{5.6\times10^6}$	$\mathbf{1.0\times10^7}$

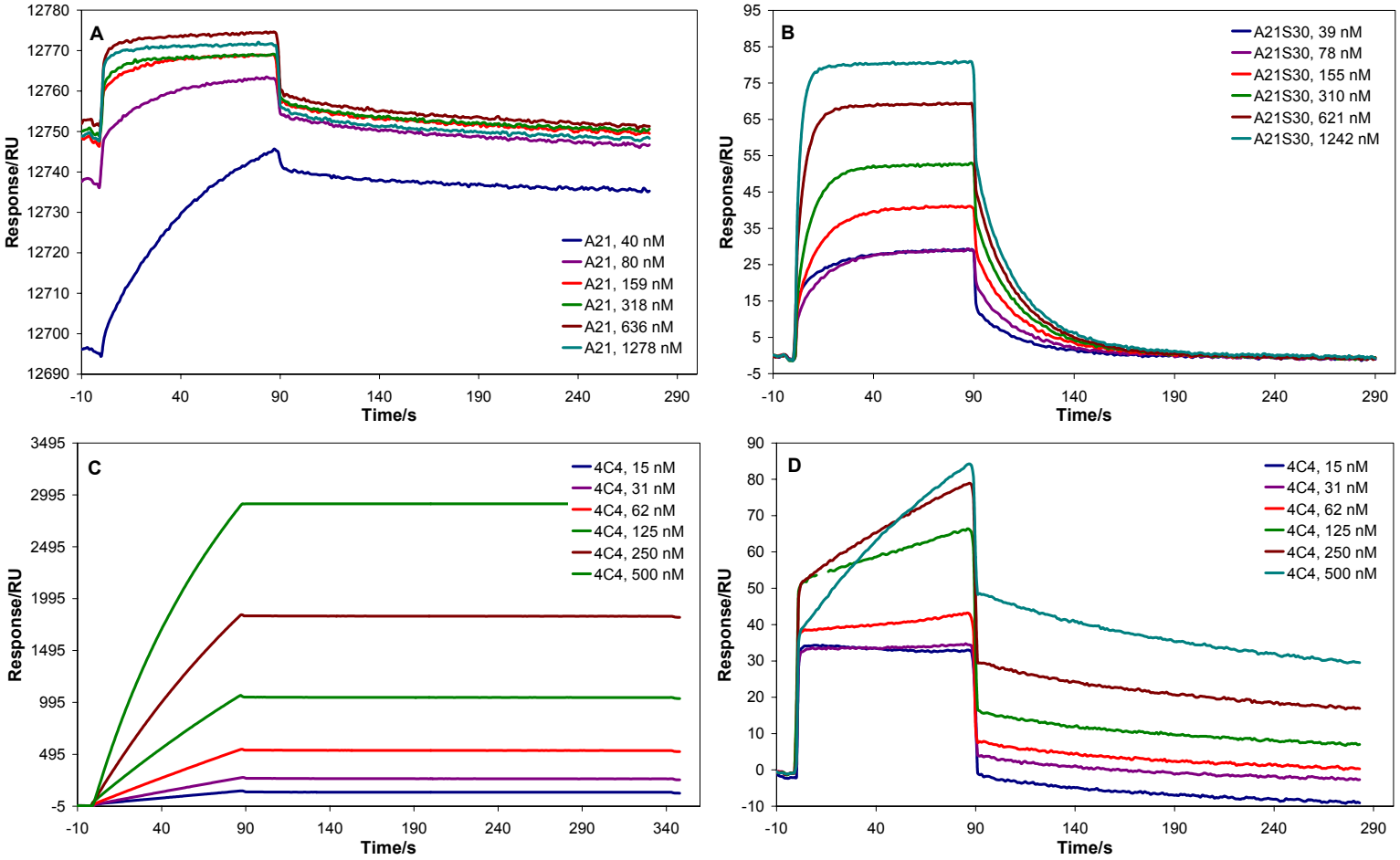

Figure 2. 10 Interactions between mAb 4C4 and peptides A21 and A21S30: ***A.*** peptide A21 *vs*. immobilised mAb (note the increasing baseline response due to incomplete surface regeneration); ***B.*** peptide A21S30 *vs*. immobilised mAb (note the high dissociation rate); ***C.*** mAb 4C4 vs. immobilised A21 (note the extremely low dissociation rate); ***D.*** mAb 4C4 vs. immobilised A21S30 (high dissociation rate).

Competition ELISA analysis of the two 21-mer peptides was also performed as described in section 2.3. Once again, peptide A21S30 was seen to be less antigenic than peptide A21 towards the three mAbs assayed (Fig. 2.11).

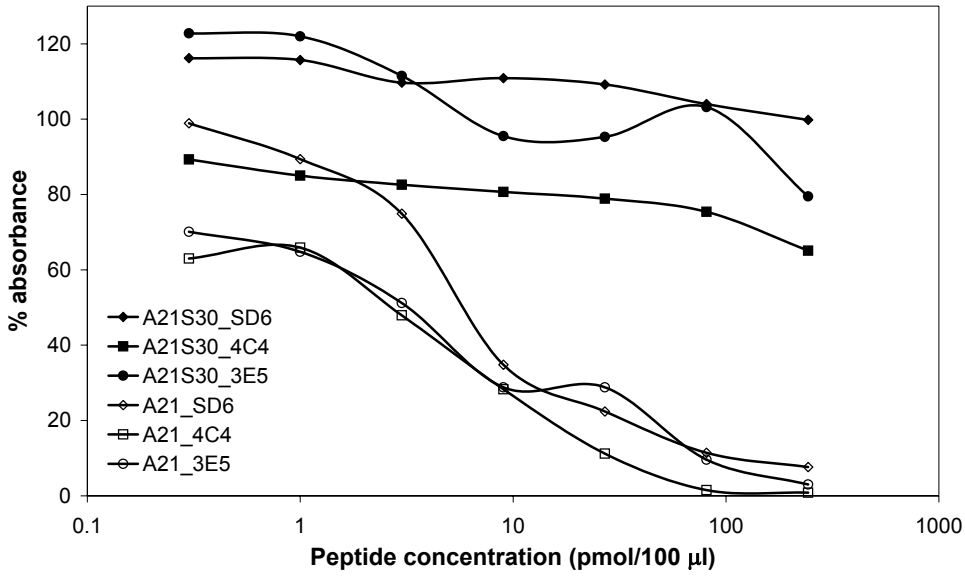

Figure 2. 11 Screening of peptides A21 and A21S30 by competition ELISA.

In summary, results from the antigenic characterisation of these 21-mer peptides showed that peptide size did not account for the low antigenicity observed for peptide A15S30 in solution. *So the question of why the C-S30 peptide sequences were less antigenic than expected from previous immunological studies*[1-7] *remained open.*

The total agreement between SPR and ELISA experiments proved that the discrepancies between our data and previous immunoenzymatic results could not come from technical or experimental artefacts.

At this point, we could only envisage a last-resource explanation, namely that in this particular case peptide conformation was responsible for the different behaviour of peptide A15S30 (or A21S30) when analysed by either ELISA/SPR or by immunodot. This remote possibility would run contrary to the general observation that the continuous antigenic site A is perfectly mimicked by linear peptides under all circumstances.

2.5 Input from parallel X-ray diffraction studies

At this point of our work we had access to X-ray diffraction studies performed by Wendy F. Ochoa and co-workers (IBMB, CSIC - Barcelona) showing that peptide A15S30 could form a complex with the Fab fragment of mAb 4C4[18]. The peptide adopted a nearly cyclic conformation in the complex, almost identical to the one observed for a similar complex with peptide A15. In the A15S30-4C4 complex, the more critical positions, residues 138 and 147, showed very few direct contacts with the antibody. Therefore, these residues influence antigenicity by altering the conformation of the peptide as a whole, rather than by local interactions. In the A15S30-4C4 complex, an additional water molecule (which could not occupy the same position in the A15-4C4 complex due to steric hindrance) was seen to bridge the side chain hydroxyl group of ^{138}Thr and the main chain oxygen atoms of ^{144}Leu and ^{147}Val (Fig. 2.12). Thus, this water molecule seemed to be a key feature in holding the compact fold of the peptide, which has been further confirmed by molecular dynamics simulations performed by the same researchers[18].

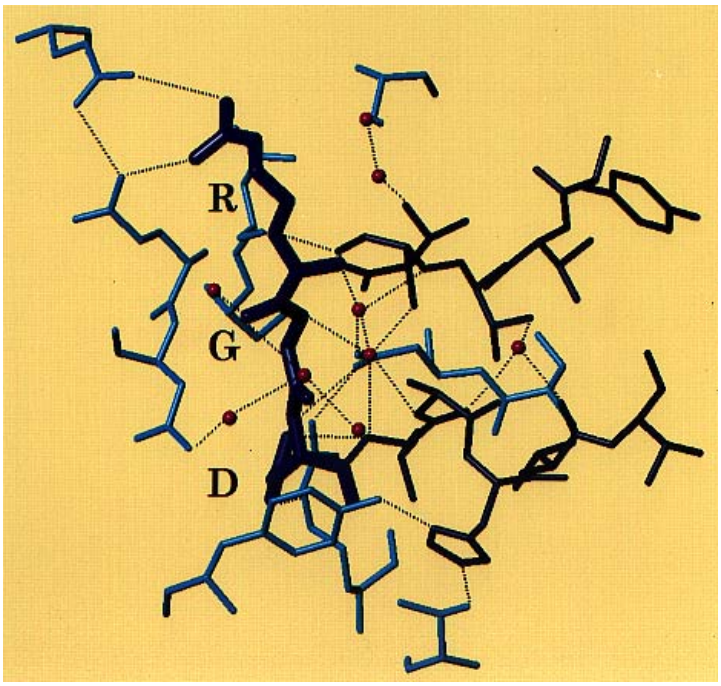

Figure 2. 12 Conformation of peptide A15S30 complexed with the Fab fragment of mAb 4C4; interactions between peptide (dark blue) and antibody (light blue) or water molecules (red spheres) are marked with dashed lines; the RGD motif is located in an open turn conformation, closely related to the one previously observed for the viral loop as part of the virion; the water molecule that bridges residues 138 (Thr side chain hydroxyl), 144 and 147 (main chain oxygen atoms) is the one further on the right side of the image. (Figure was provided by Ms. Wendy F. Ochoa).

2.6 Effect of conformation in the antigenicity of C-S30 peptides

When earlier FMDV C-S30 studies, recent X-ray diffraction data and our own results on antigenicity of C-S30 peptides are all brought together, it seems plausible that the apparent discrepancies between the former and the latter data are due to factors such as distinct conformations of the antigenic site under the different assay systems employed. Therefore, we decided to analyse the effect of introducing conformational constraints in the C-S30 peptides. For that purpose, two additional cyclic peptides (cyc16S30 and cyc16^{147}Val) were synthesised.

2.6.1 Synthesis of peptides cyc16S30 and cyc16^{147}Val

The design and synthesis of these cyclic peptides was based on previous research in our group, involving the same type of constructs based on the GH loop sequence belonging to the C-S8c1 viral strain. Cyclic versions of the viral antigenic site were formed by intra-molecular disulphide formation between N- and C-terminal cysteine residues added to the sequences. An extra 6-aminohexanoic acid (Ahx) residue was also included to give some flexibility to the constructs, so that the known disordered structure of the viral loop could be better mimicked[19]. Production of these cyclic peptides relied on the synthesis and purification of the corresponding linear bis-thiol precursors (A15S30 and A16^{147}Val) using methods similar to those previously described in section 2.1, followed by air oxidation of the thiol groups at pH 8 and high peptide dilution (Fig. 2.13)[20]. Cyclization was monitored by HPLC and the qualitative Ellman[21] assay (see Materials & Methods), reaching completion within one hour (Fig. 2.14). Cyclic peptides were then lyophilised without further purification. General data on the synthesis and cyclization of these peptides are presented in Table 2.7.

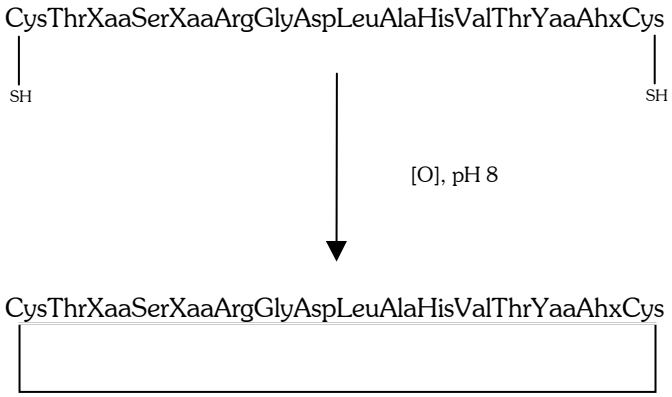

Figure 2. 13 Oxidation of bis-thiol precursors to cyclic peptides cyc16S30 (Xaa=Thr, Yaa=Ala) and cyc16^{147}Val (Xaa=Ala, Yaa=Thr); air oxidation was performed at pH 8 and high dilution (50 μM) to favour intra-molecular cyclization.

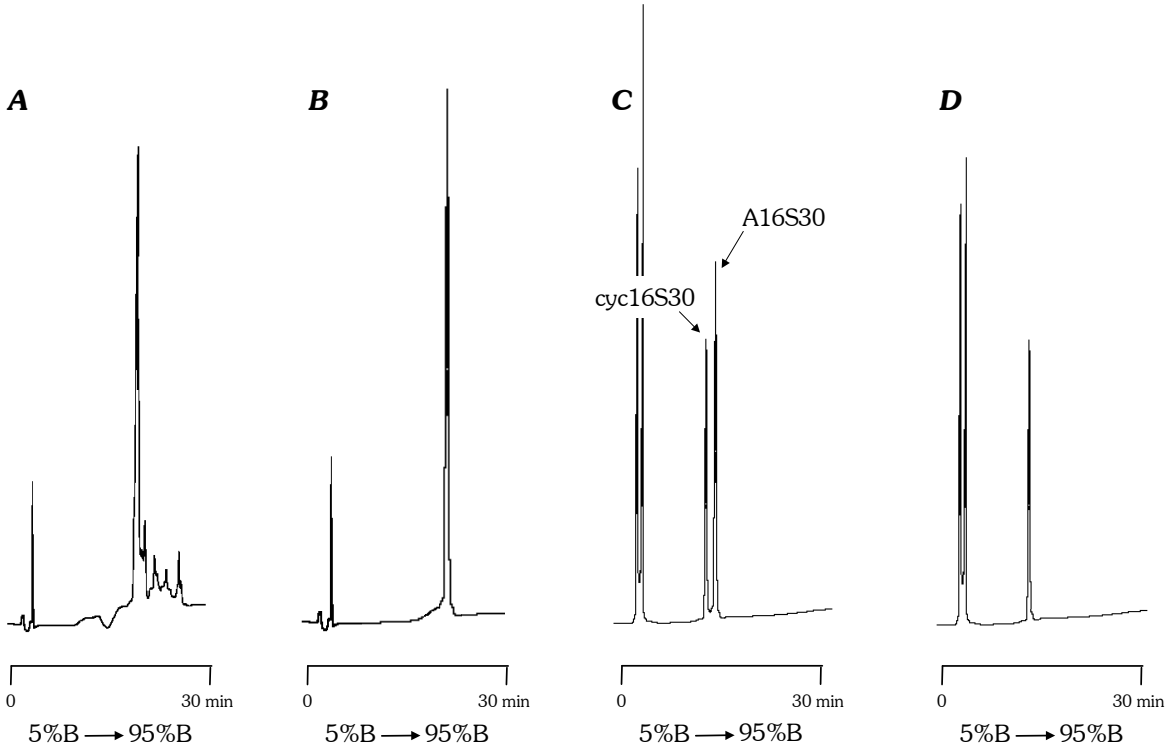

Figure 2. 14 HPLC profiles showing both linear and cyclic forms of the different steps in the synthesis of cyc16S30; ***A.*** crude A16S30 (bis-thiol form), ***B.*** MPLC-purified A16S30, ***C.*** air oxidation at 30 min, ***D.*** oxidation at 1 hour.

Table 2.7 Synthesis of the C-S30 cyclic peptides and their bis-thiol precursors.

Peptide	***Global yield (%)***	***Purity (%HPLC)***	***MW found***	***MW expected***	***AAA****
A16S30	37	97	1647.2	1647	Asp, 1.02 (1); Ser, 1.02 (1); Gly, 0.99 (1); Ala, 1.99 (2); Leu, 0.98 (1)
cyc16S30	82	95	1645.4	1645	Asp, 0.99 (1); Ser, 1.07 (1); Gly, 0.97 (1); Ala, 1.99 (2); Leu, 0.99 (1)
A16^{147}Val	34	94	1617.9	1618	Asp, 1.05 (1); Ser, 1.01 (1); Gly, 0.99 (1); Ala, 2.76 (3); Leu, 0.97 (1)
cyc16^{147}Val	85	93	1615.9	1616	Asp, 1.07 (1); Ser, 1.04 (1); Gly, 0.93 (1); Ala, 2.78 (3); Leu, 0.96 (1)

*Relative amino acid proportions given by AAA are followed by the expected value in parenthesis.

2.6.2 Antigenic evaluation of cyclic C-S30 peptides using SPR

The affinities of the cyclic peptides towards the three anti-site A mAbs were measured by SPR analysis, both with peptide as analyte and as immobilised ligand (Table 2.8 and Fig. 2.15).

Table 2.9 Interactions between peptides cyc16S30 and cyc16^{147}Val and anti-site A mAbs.

Peptide / ***mAb***		***as analyte***		***immobilised on the chip***	
		cyc16S30	*cyc16^{147}Val*	*cyc16S30*	*cyc16^{147}Val*
SD6	$k_a/M^{-1}s^{-1}$	$7.2x10^4$	$1.8x10^5$	$2.0x10^4$	$1.5x10^4$
	k_d/s^{-1}	$1.8x10^{-2}$	$4.5x10^{-3}$	$4.1x10^{-3}$	$1.1x10^{-3}$
	K_A/M^{-1}	***$4.0x10^6$***	***$4.1x10^7$***	***$4.8x10^6$***	***$1.3x10^7$***
4C4	$k_a/M^{-1}s^{-1}$	$5.0x10^5$	$1.7x10^5$	$9.3x10^3$	$1.5x10^4$
	k_d/s^{-1}	$3.5x10^{-3}$	$5.0x10^{-3}$	$8.9x10^{-5}$	$2.6x10^{-4}$
	K_A/M^{-1}	***$1.4x10^8$***	***$3.3x10^7$***	***$1.1x10^8$***	***$5.0x10^7$***
3E5	$k_a/M^{-1}s^{-1}$	$4.5x10^5$	$1.6x10^5$	$1.0x10^4$	$1.0x10^4$
	k_d/s^{-1}	$5.4x10^{-3}$	$2.9x10^{-3}$	$2.0x10^{-4}$	$4.1x10^{-4}$
	K_A/M^{-1}	***$8.4x10^7$***	***$5.5x10^7$***	***$5.0x10^7$***	***$2.5x10^7$***

Before discussing the SPR data of the cyclic peptides, it must be re-emphasised that analyses using mAb as analyte were not subject to optimisation and, therefore, data from such analyses should be regarded as purely comparative. In fact, kinetic constants in Table 2.9 show that mass-transport limitations are probably occurring when mAb is used as analyte, since rate constants measured under this analysis configuration are lower than when the small peptides are the analytes[11-13]. However, since both rate constants seem to be affected by mass-transport artefacts to a similar extent, the affinities displayed are within the same order of magnitude as those measured in the reverse configuration and, furthermore, the antigenicity ranking of the peptides is maintained in both analysis formats.

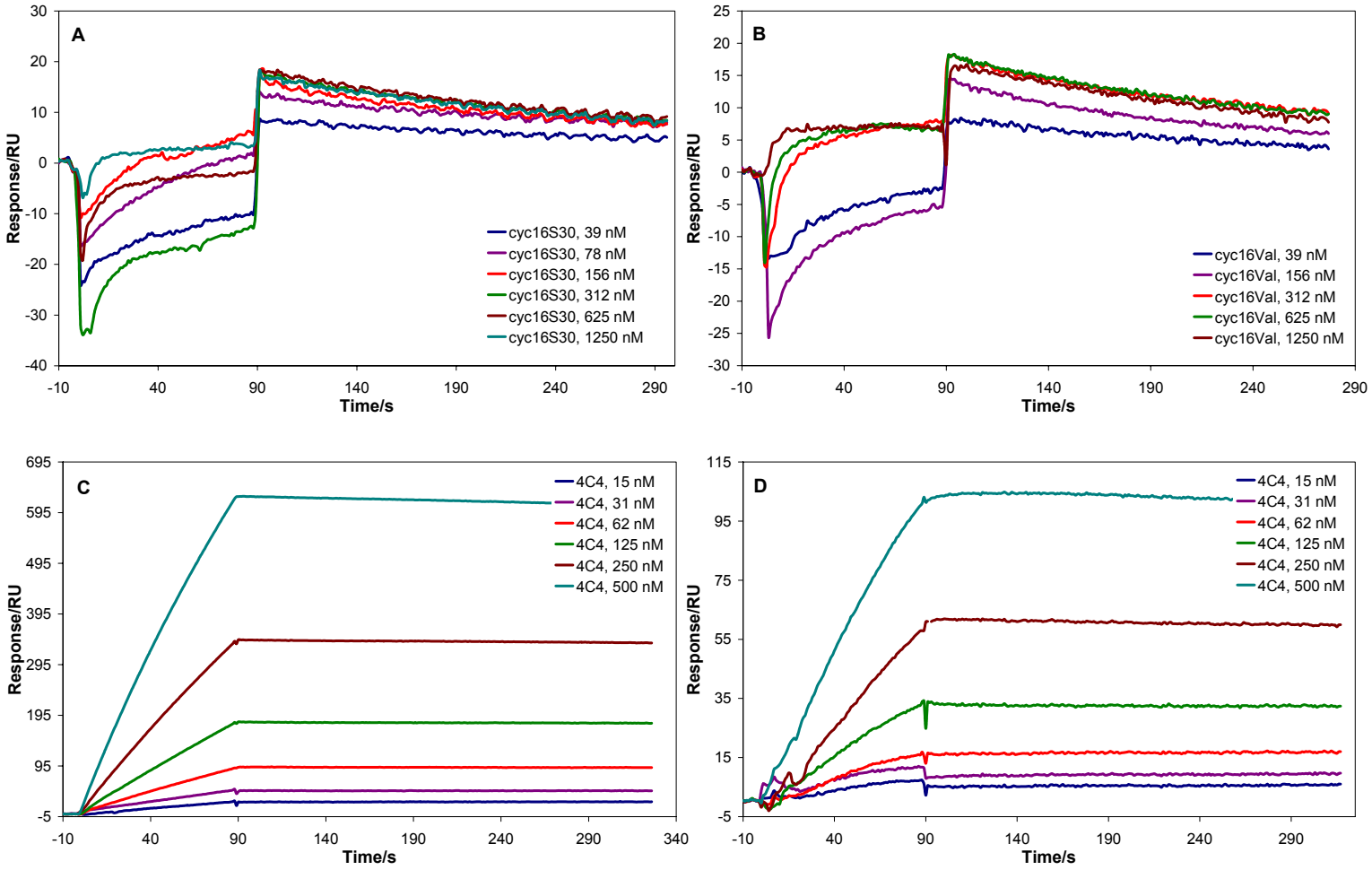

Figure 2. 15 Sensorgrams of the SPR kinetic analysis of the interactions between mAb 4C4 and: peptide cyc16S30 as analyte (A) and as immobilised ligand (C); peptide cyc16^{147}Val as analyte (B) and as immobilised ligand (D).

Data in Table 2.9 show that cyclic versions of peptides A15S30 (*i.e.*, peptide cyc16S30) and A15(147Val) (*i.e.*, peptide cyc16^{147}Val) are clearly more antigenic than their linear counterparts against all three mAbs. Further, the increase in affinity is reflected in both association and, especially, dissociation rate constants, indicating that cyclic peptides bind more readily to the mAbs and that the resulting complexes are stabilised to a greater extent. A similar result had been observed by M. L. Valero and co-workers in the analysis of the interactions between mAb SD6 and both peptide A15 and its corresponding cyclic disulphide analogue (AhxA16SS)[19]. In this previous study, an increase of about one order of magnitude in mAb affinity was observed upon peptide cyclization (K_A from 1.9×10^7 to 1.2×10^8 M^{-1}), but almost exclusively due to an increase in association rate constant (k_a from 3.7×10^3 to 2.6×10^4 $M^{-1}s^{-1}$). This indicated that, despite the easier entry of the cyclic peptide into the mAb paratope, the final complex had the same half-life as the one formed with the linear analogue (k_d was 2.2×10^{-4} and 2.0×10^{-4} s^{-1} for the cyclic and linear peptides, respectively).

The most striking observation made with our cyclic peptides corresponding to FMDV C-S30 and to a hypothetical Leu147→Val mutant (a field isolate with such single-point replacement has not yet been isolated) was the fact that, while the C-S30 sequence was less antigenic than the ^{147}Val mutant towards mAb SD6, this ranking was inverted when the other two mAbs were considered (the results with mAb 4C4 being the most significant). This was precisely what had been observed in earlier immuno-enzymatic studies of field isolate C-S30 as well as of KLH conjugates of site A peptides displaying either the corresponding four replacements or the single Leu147→Val substitution. Further, this was the first evidence, using small peptides, of the reversion observed in 4C4 – antigen affinity when both Ala138→Thr and Leu147→Val replacements were brought together. Additionally, these results confirmed what had been postulated by W. F. Ochoa and co-workers, concerning the fact that residues ^{138}Thr and ^{147}Val in the A15S30-4C4 complex have only minor contacts with the antibody paratope and, thus, differences in binding affinities observed for peptides with replacements at these positions would be due to reduced stability of such peptides in the "mAb-recognisable" conformation[18].

A question still remained, however: *peptide A15S30 can be crystallised in complex with antibody 4C4, so both molecules can undergo a considerable induced fit to form a stable complex. Therefore, would prolonged (e.g., overnight) incubation of peptide with antibody, both species in solution, result in higher affinities than those measured in kinetic SPR or competition ELISA assays?*

2.7 Antigenic evaluation of C-S30 peptides through solution affinity SPR analysis

2.7.1 Basic concepts[22,23]

Measurement of affinity in solution with SPR biosensors is based on the determination of the free concentration of one of the interactants in equilibrium mixtures. Measurements are made on known concentrations of the free interactant for a standard curve to be built and also on the equilibrium mixtures for determination of affinity. If binding in solution is written as:

$$A + B \rightleftharpoons AB$$

the experiment is designed so that a constant concentration of B is incubated with a series of known concentrations of A and, then, SPR is used to measure the remaining free concentration of B in solution (Fig. 2.16). Such measurement is performed on a sensor chip surface where a specific ligand for B (A') had been previously immobilised and on which a calibration curve using known concentrations of B had been built. The affinity constant can then be calculated with the BIAEvaluation software[24], where the variation of free B with the concentration of A is fitted to the equation:

$$\frac{[B]-[A]-K_D}{2}+\sqrt{\frac{([A]+[B]+K_D)^2}{4}-[A]\times[B]} \qquad (2.1)$$

In the particular case of antigen – antibody interactions (taking, for instance, B for antibody and A for antigen), one should ensure that reactions take place at a 1:1 stoichiometry. Thus, antibody Fab fragments instead of the whole immunoglobulin must be employed. Fab fragments of the relevant antibodies were produced by digestion with papain, as described under Materials & Methods[B] (section 4.3.1.3).

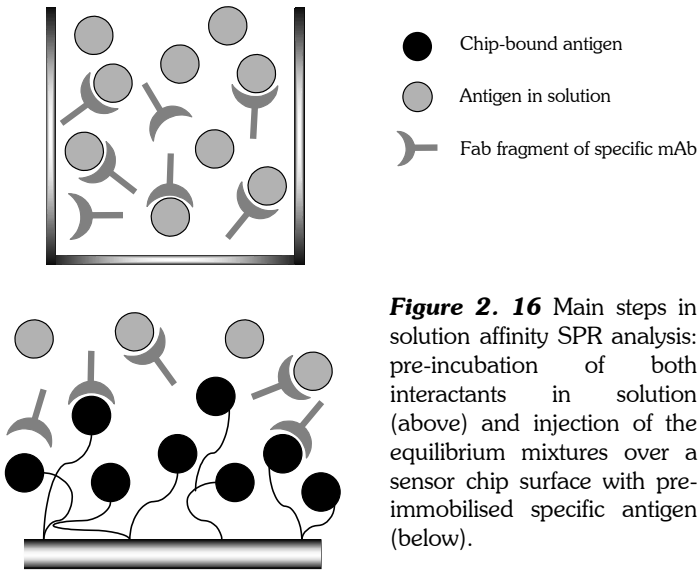

Figure 2. 16 Main steps in solution affinity SPR analysis: pre-incubation of both interactants in solution (above) and injection of the equilibrium mixtures over a sensor chip surface with pre-immobilised specific antigen (below).

[B] Purified Fab of SD6 was kindly supplied by Dr. Esteban Domingo and Ms. Mercedes Dávila (CBMSO – UAM, Madrid); Fab 4C4 was a kind gift of Dr. Nuria Verdaguer and Ms. Wendy F. Ochoa (IBMB – CSIC, Barcelona); Fab from mAb 3E5 was prepared by digestion of mAb isolated from ascitic fluid kindly supplied by Dr. Emiliana Brocchi (IZSLE, Brescia – Italy).

The main steps in antibody digestion and Fab purification were monitored by SDS-PAGE (Fig. 2.17).

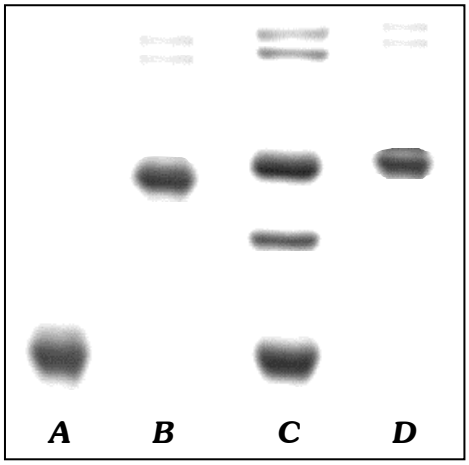

Figure 2. 17 SDS-PAGE monitoring (at 12% acrylamide) of the digestion and purification of the Fab fragment of mAb 3E5; lanes ***A*** and ***B***: purified mAb 4C4 and its corresponding Fab fragment, used instead of MW protein standards; lane ***C***: papain digestion of mAb 3E5 at 3 h of reaction; starting mAb, plus Fab_2 and Fab products can be distinguished; lane ***D:*** Fab fragment of mAb 3E5 after a two-step (affinity and gel filtration chromatography) purification.

Solution affinity SPR analysis relies on concentration measurements. In the SPR biosensor, concentration measurements are based either on binding level (avoiding bulk refractive index contributions) or on binding rate determinations. Under conditions of limiting mass transfer of analyte to the surface, the initial binding rate is independent of ligand density and interaction kinetics, being exclusively determined by analyte concentration and diffusion characteristics. In the present study, we were able to see that SPR analyses with immobilised peptide and antibody as analyte were influenced by mass-transport artefacts even at flow rates as high as 60 µl/min (sections 2.2.3, 2.4.2 and 2.6.2). Thus, free Fab concentrations in the present study had to be derived from initial binding rate measurements at 5 µl/min on sensor chips with peptide A15 (0.3 ng/mm^2) pre-immobilised by standard procedures (see Materials & Methods, section 4.3.1.3). Binding rates were taken from curve slopes at a given injection time, chosen as the earliest possible where the influence of bulk refractive index or other artefacts at injection plugs would be negligible.

It could be argued that there was no evidence that the Fab – A15 interactions were 100% diffusion-controlled. Nevertheless, all measurements were performed on the same A15 surface and the analyte (Fab) was always the same for each data set, so antigenicity ranking of the peptide analogues screened under these conditions is totally meaningful.

The dependence of the measured free Fab concentration on antigen concentration gives an inhibition curve that can be fitted to Eq. 2.1 (BIAEvaluation general fit→solution affinity model) so that affinity is calculated (as either K_A or its reciprocal K_D). However, the influence of immobilised antigen (A15) on free Fab concentration measurements is not taken into account when fitting data as described; in fact, the immobilised peptide is competing with the soluble analogue for the same Fab molecules as in competition ELISA. The Cheng and Prusoff's formula (Eq. 2.2)[25] can be used to obviate this problem:

$$K_i = 1 + \frac{K'_A [B]}{IC_{50}} \qquad (2.2)$$

where K_i is the "real" affinity for the interaction of A and B in solution, K'_A is the affinity for the interaction of B with immobilised A' and IC_{50} is the concentration of A causing a 50% drop in the total concentration of B.

2.7.2 Results

Injection of known Fab (SD6, 4C4 and 3E5) standards on the A15 surface allowed the building of calibration curves (Fig. 2.18), which were subsequently employed in the determination of Fab molecules that remained free after overnight incubation with peptide antigens in solution.

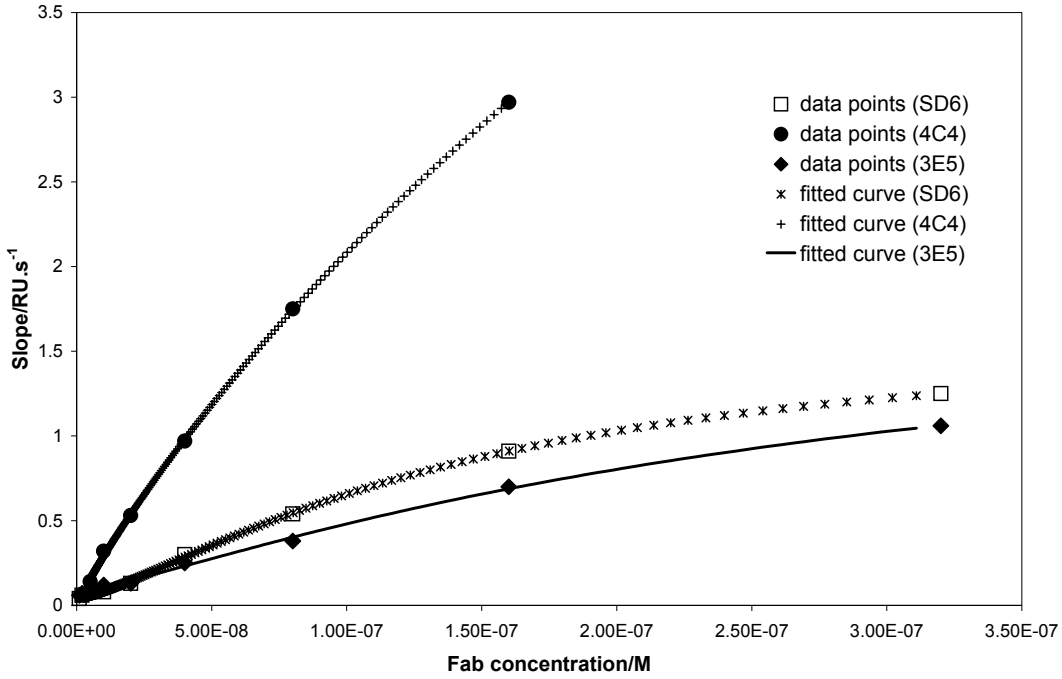

Figure 2. 18 Plots of *initial binding rate/RU.s^{-1} vs. Fab concentration (M)* for the three antibodies employed in the present study. Measurements were made at a 5 µl/min flow rate on a 0.3 ng/mm^2 A15 surface; data points were fitted to a four-parameter equation using BIAEvaluation software in order to build the corresponding calibration curves.

The quantification of remaining free Fab in solution for each incubated mixture (where Fab total concentration is constant and peptide antigen concentrations varied) allowed to build inhibition curves (Fig. 2.19) from which the peptide – antibody solution affinities were calculated, either through direct fitting to the BIAEvaluation solution affinity model (Eq. 2.1) or using the Cheng & Prusoff's formula (Eq. 2.2). Results are summarised in Table 2.9.

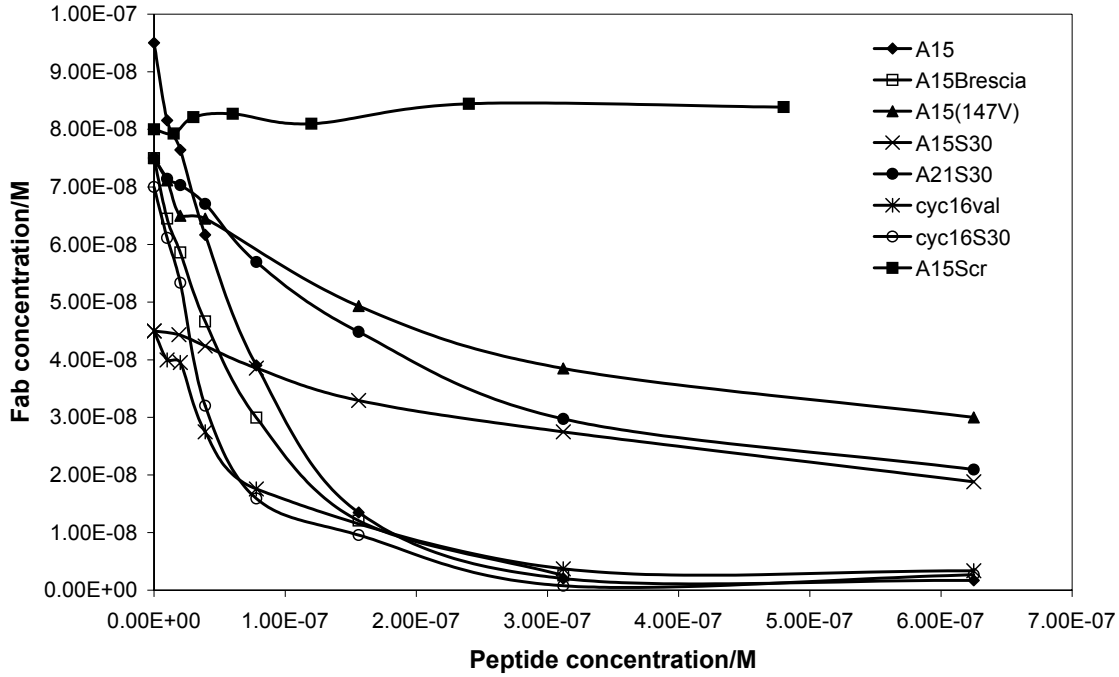

Figure 2. 19 Inhibition curves obtained in the SPR analysis of the interactions between Fab 4C4 and peptides A15, A15Brescia, A15(147Val), A15S30, A21S30, cyc16S30, cyc16^{147}Val and A15Scr in solution; a constant total Fab concentration was used and competitor peptide concentrations were varied from 0 to 625 nM.

Table 2.9 Affinity data of interactions between peptides and mAbs in solution.

Fab	Peptide	K_A (solution affinity fit)[a]/M^{-1}	K_i (Cheng & Prusoff's)[b]/M^{-1}	***K_A (kinetic analysis)[c]/M^{-1}***
	A15	4.3×10^{7}	***6.3×10^{7}***	5.4×10^{7}
	A15(147V)	3.6×10^{6}	***4.5×10^{6}***	1.0×10^{7}
	A15Brescia	4.3×10^{7}	***6.5×10^{7}***	1.2×10^{7}
SD6	A15S30	6.0×10^{5}	***ND***	4.3×10^{5}
	A21S30	1.6×10^{6}	***ND***	3.0×10^{6}
	cyc16S30	2.8×10^{6}	***7.5×10^{6}***	4.0×10^{6}
	cyc16^{147}Val	5.5×10^{7}	***5.0×10^{7}***	4.1×10^{7}
	A15	8.2×10^{7}	***2.0×10^{8}***	1.9×10^{8}
	A15(147V)	3.8×10^{6}	***2.8×10^{7}***	2.2×10^{6}
	A15Brescia	5.5×10^{7}	***1.5×10^{8}***	1.6×10^{8}
4C4	A15S30	2.3×10^{6}	***1.1×10^{7}***	2.0×10^{6}
	A21S30	5.2×10^{6}	***3.8×10^{7}***	5.6×10^{6}
	cyc16S30	1.4×10^{8}	***1.8×10^{8}***	1.4×10^{8}
	cyc16^{147}Val	2.7×10^{7}	***8.2×10^{7}***	3.3×10^{7}
	A15	1.6×10^{8}	***2.0×10^{8}***	9.4×10^{7}
	A15(147V)	4.5×10^{6}	***2.8×10^{7}***	6.6×10^{6}
	A15Brescia	6.5×10^{7}	***1.1×10^{8}***	1.0×10^{8}
3E5	A15S30	2.1×10^{6}	***8.2×10^{6}***	4.5×10^{6}
	A21S30	2.9×10^{6}	***1.1×10^{7}***	5.6×10^{6}
	cyc16S30	4.4×10^{7}	***1.1×10^{8}***	8.4×10^{7}
	cyc16^{147}Val	4.5×10^{7}	***8.5×10^{7}***	5.5×10^{7}

[a] Direct curve fitting with the BIAEvaluation software.
[b] Application of the Cheng & Prusoff's formula.
[c] Data from previous SPR kinetic assays.
ND, not determined.

2.7.3 Discussion

SPR measurement of affinities of C-S8c1, C_1-Brescia and C-S30 peptides for anti-site A mAbs SD6, 4C4 and 3E5 provided a conclusive confirmation of the data discussed in the present chapter. Indeed, as can be seen in Fig. 2.20 and Table 2.9, antigenicity rankings observed for these interactions were in good agreement with those previously obtained by competition ELISA and kinetic SPR analysis. Peptide A15S30 was less antigenic than its counterparts from strains C-S8c1 (peptide A15) or C_1-Brescia (A15Brescia). At the same time, important differences were observed and are discussed in the following paragraphs.

i) Solution affinities obtained by curve fitting or by the Cheng & Prusoff's formula

Comparing the affinities in Table 2.9 as obtained by solution affinity fit or by the Cheng & Prusoff's formula, the influence of immobilised antigen A15 becomes quite evident. Thus, Eq. 2.1 describes phenomena such as those occurring in competition ELISA. In this case, peptides with lower antigenicity will be the most affected by the immobilised antigen competitor and fitted affinities will be lower than affinities determined in solution. In contrast, the Cheng & Prusoff's formula (Eq. 2.2) allows to obtain data independent from the immobilised antigen and major differences between both methods of affinity calculation can be observed for the least antigenic peptides A15(147V), A15S30 and A21S30 towards mAbs 4C4 and 3E5. Differences of about one order of magnitude can be found in these cases, relative to affinities calculated by direct fit of the inhibition curves.

ii) Solution affinity versus kinetic SPR data

Comparing affinity data calculated from the inhibition curves using Eq. 2.2 with previous data obtained by kinetic SPR analysis, an excellent agreement is observed with three important exceptions: peptides A15(147V), A15S30 and A21S30 (towards mAbs 4C4 and 3E5). Even though relative ranking of all antigens is maintained, an increase in affinity of about one order of magnitude is measured in solution equilibrium experiments involving these peptides. The fact that such observation is more pronounced for these three particular peptide mutants appears to be quite significant. Indeed, it seems that when antigen and antibody are allowed to interact overnight both free in solution, they can rearrange so that more stabilised complexes are formed. Thus, the lower affinities measured in kinetic SPR analysis would possibly be due to interaction times (1.5 min) too small for such conformational changes to be detected. This ability of the C-S30 GH loop to rearrange into a mAb-recognisable structure, leading to stable antibody-antigen complexes, could be the basis for the recognition and neutralisation of FMDV C-S30 by mAb 4C4.

iii) A role for peptide conformation

The above observations are further supported by the modulation of peptide antigenicity upon cyclization. Both four-point and one-point (^{147}Leu→Val) replaced sequences produced important increases in mAb affinities when presented as cyclic peptides. Particularly in the case of mAb 4C4, it was observed that the cyclic C-S30 sequence was about one order of magnitude more antigenic than the cyclic one-point mutant ^{147}Leu→Val, which confirms previous studies suggesting a positive reversion in the antigenicity of the four-point mutant[1-7]. These observations have important implications *vis à vis* the simplistic view of continuous antigenic sites as conformation-independent. If this was in fact the case, peptide cyclization would have only minor effects on antigenicity. Further, the loss of antigenicity due to amino acid replacements in positions that are not in direct contact with the antibody paratope[18] (*e.g.*, ^{138}Ala→Thr and ^{147}Leu→Val in linear peptides) cannot be easily explained by factors other than peptide conformation.

2.8 Two-dimensional proton nuclear magnetic resonance studies of C-S30 peptides[26]

Most linear and many cyclic peptides possess a high conformational flexibility, meaning that they can adopt a fairly large set of interconvertible conformations in solution. In a few favourable cases, the population of one conformer is large enough to be distinctly detected by spectroscopy. Among the techniques commonly employed for the detection and identification of peptide conformation such as circular dichroism, Raman spectroscopy, FT-IR and NMR, the latter has a clear advantage in that it allows not only the global detection of the preferred structure, but also the characterisation of the individual amino acid residues defining such structure. Thus, it provides a picture of peptide folding in aqueous solution, which is desirable when searching for structure – activity relationships.
Due to their natural abundance, gyromagnetic constant and localisation in peptides, protons are the best probes for peptide conformational NMR studies. Although a simple one-dimensional NMR spectrum of the peptide should always be obtained in order to check for peptide purity, concentration or aggregation, the level of complexity is usually too high for a complete assignment. So, two-dimensional NMR experiments are needed for a full and unequivocal proton assignment in peptide studies.
Peptides A15S30 and cyc16S30 were both studied by 2D – ^{1}H NMR in solution, in an attempt to define secondary structure elements that could explain the antigenic features of both peptides. NMR experiments (TOCSY[27], NOESY[28] and ROESY[29]) were carried out both in aqueous solution and in the presence of the structuring agent trifluoroethanol, as described under Materials & Methods (section 4.4.1).

2.8.1 Basic concepts

2D – ^{1}H NMR spectra of peptides are interpreted according to the *sequential assignment method* developed by Wüthrich for proteins[27]. The first step in the procedure relies on the *total correlation scalar experiment* (TOCSY), in which peaks are detected for protons that can correlate with each other by means of a magnetisation transfer sequence involving, at each step, H – H couplings. This allows the identification of each amino acid residue independently from all the others in the sequence, since magnetisation cannot be transferred through the amide bond from one residue to the following one. Thus, each amide proton (H^N) will be correlated with all other protons from the same spin system; the number and chemical shift of such protons provide an identification of the amino acid residue in question. If the peptide includes an amino acid residue that is unique in the whole sequence, the assignment is immediate and unequivocal. However, if a certain amino acid residue is repeatedly present along the sequence, it will be necessary to carry out another kind of NMR experiment where protons from different amino acid residues are correlated. Such correlation is based on *nuclear Overhauser effect* (NOE) experiments (NOESY[28], ROESY[29]). The NOE arises from the dipolar relaxation that occurs between two nuclei that are spatially close to each other,

regardless of their belonging or not to the same spin system. An NOE between a pair of protons is, therefore, observed when there is a population of peptide structures where both nuclei are within 4.5 Å from each other. Thus, when all residues are attributed a set of signals in the TOCSY spectrum, the second step will be the use of NOE experiments to establish connectivities among them. This will be possible if sequential distances such as $d_{\alpha Ni,i+1}$, $d_{Nni,i+1}$, $d_{\beta Ni,i+1}$, etc., can be observed, *i. e.*, correlations between proton H^{α} of residue *i* with H^{N} of residue *i+1*, or H^{N} of residue *i* with H^{N} of residue *i+1,* or H^{α} of residue *i* with H^{N} of residue *i+1*, respectively. Since the α proton of a given residue is usually close in space to the H^{N} of the following residue, sequential $d_{\alpha Ni,i+1}$ NOEs are useful to assign the amino acid sequence.

Given the slow time-scale of NMR spectroscopy relative to optical spectroscopy, one must keep in mind that NMR spectral parameters are all averaged. Thus, all conformational information provided by NMR corresponds to the average of all structures adopted by the peptide in solution. Of the several parameters that can be used in NMR peptide structural studies, only *conformational chemical shifts* and *NOEs* have been considered in the present work.

Chemical shifts are the most easily measured NMR parameters and are quite susceptible to subtle changes in the chemical environment of the proton. The large number of protein structures assigned by NMR made possible a statistical study correlating differences in chemical shifts with peptide secondary structure. The most useful chemical shift differences have been found to be those between the H^{α} of folded and random coil structures, the latter ones derived from model oligopeptides. Thus, H^{α} *conformational chemical shift differences* (defined as $\Delta\delta H^{\alpha}=\delta_{exp} - \delta_{\text{random coil}}$) are found to be negative for helices (average, - 0.39 ppm) and β turns, and positive for β sheets (average, + 0.37 ppm). NOEs usually provide the most unambiguous information about peptide structure. The sole observation of a NOE between two protons implies that there are conformational populations in which these two protons are spatially close (d ≤ 4.5 Å), independently of their being or not close in the primary sequence. Energy studies on the conformational space of proteins allow to establish NOE patterns that correlate with peptide secondary structure. A general guide for structural interpretation of NOEs is presented in Table 2.10.

Table 2.10 Useful NOEs for the identification of peptide secondary structure elements.

NOE	***Structure***				
	Helix		***β sheet***	***β turn***	
	α	3_{10}		***I***	***II***
$d_{\alpha Ni,i+1}$	✔✔	✔✔	✔✔✔	✔✔	✔✔✔
$d_{NNi,i+1}$	✔✔✔	✔✔✔	✔	✔✔✔ *(2)*	✔✔✔ *(1)*
$d_{NNi,i+2}$	✔	✔	✘	✔✔	✔
$d_{\alpha Ni,i+2}$	✔	✔✔	✘	✔✔	✔✔
$d_{\alpha Ni,i+3}$	✔✔	✔✔	✘	✔	✔
$d_{\alpha Ni,i+4}$	✔	✘	✘	✘	✘
$d_{\alpha\beta i,i+3}$	✔	✔	✘	✘	✘

✔ - expected NOE (the number of ticks corresponds to the expected intensities); ✘ - not observed.

2.8.2 Results

Sequence assignment based on TOCSY and NOESY/ROESY spectra is shown in Fig. 2.20 for both A15S30 and cyc16S30 peptides in water. Chemical shifts observed for both peptides, in water as well as in 30% TFE, are presented in Table 2.11.

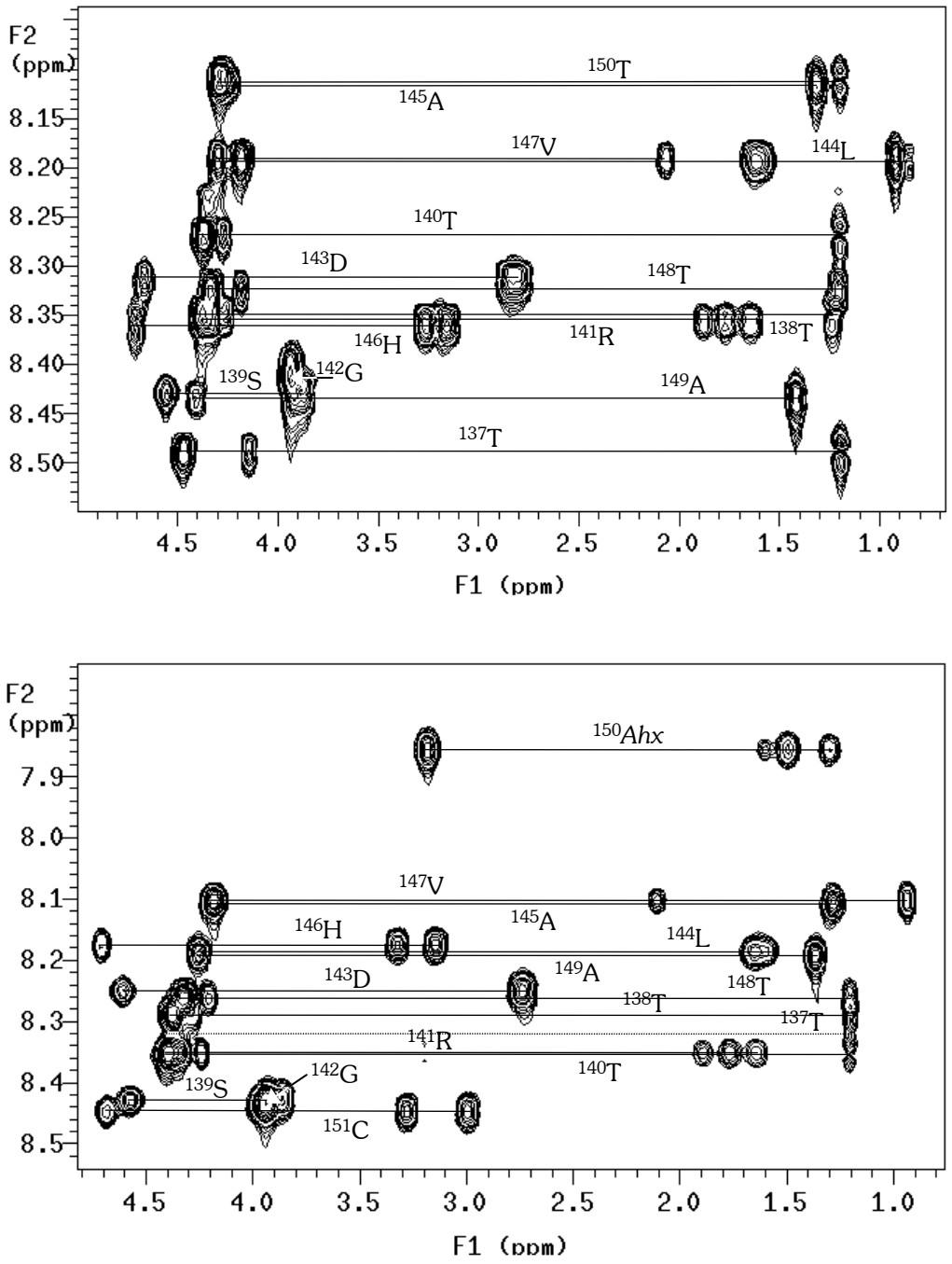

Figure 2. 20 Expansion of the TOCSY experiments (70 ms) of peptides A15S30 (above) and cyc16S30 (below) performed at 25 °C in water; the different spin systems are indicated and were assigned upon analysis of TOCSY, NOESY and ROESY spectra.

Table 2.11 Chemical shifts (ppm) measured in the 2D – ^{1}H NMR study of peptides A15S30 and cyc16S30 in water and in 30% TFE at 25 °C.

Residue	***A15S30***								***cyc16S30***							
	H_2O				***30% TFE***				***H_2O***				***30% TFE***			
	H^N	H^α	H^β	Other	H^N	H^α	H^β	Other	H^N	H^α	H^β	Other	H^N	H^α	H^β	Other
^{136}Tyr/Cys	nd	4.32	3.15 3.19	nd	nd	4.32	3.13 3.20	nd	nd	4.48	3.34 3.23	ne	nd	4.48	3.40 3.26	ne
^{137}Thr	8.49	4.47	4.15	1.20	8.40	4.52	4.20	1.24	8.34	4.42	4.25	1.20	8.03	4.22	4.18	1.28
^{138}Thr	8.36	4.32	4.25	1.24	8.25	4.41	4.32	1.28	8.29	4.38	4.28	1.20	8.25	4.45	4.31	1.25
^{139}Ser	8.43	4.55	3.86 3.92	ne	8.33	4.60	3.91 3.98	ne	8.43	4.57	3.88	ne	8.33	4.60	3.96 3.90	ne
^{140}Thr	8.27	4.37	4.27	1.20	8.18	4.40	4.31	1.25	8.36	4.40	4.24	1.20	8..18	4.43	4.33	1.24
^{141}Arg	8.35	4.32	1.89 1.77	3.30 1.66	8.28	4.30	1.90 1.80	3.20 1.70	8.36	4.34	1.89 1.76	3.22 1.64	8.28	4.36	1.93 1.80	3.22 1.70
^{142}Gly	8.40	3.93	ne	ne	8.32	3.95	ne	ne	8.44	3.94	ne	ne	8.34	3.97	ne	ne
^{143}Asp	8.32	4.66	2.85 2.80	ne	8.21	4.65	2.86	ne	8.25	4.61	2.73	ne	8.15	4.67	2.83	ne
^{144}Leu	8.19	4.29	1.61	0.92 0.85	8.08	4.26	1.71	0.95 0.90	8.16	4.24	1.66	0.92 0.84	8.14	4.24	1.69	0.95 0.90
^{145}Ala	8.12	4.23	1.32	ne	8.02	4.22	1.38	ne	8.10	4.18	1.28	ne	8.03	4.20	1.34	ne
^{146}His	8.36	4.71	3.15 3.26	nd	8.09	4.67	3.37 3.23	nd	8.16	4.70	3.30 3.14	nd	8.05	4.69	3.43 3.20	nd
^{147}Val	8.19	4.18	2.07	0.92	8.05	4.12	2.20	1.00	8.09	4.17	2.10	0.94	8.04	4.18	2.19	1.00
^{148}Thr	8.33	4.33	4.19	1.21	8.07	4.37	4.29	1.25	8.26	4.32	4.21	1.20	8.07	4.36	4.29	1.24
^{149}Ala	8.44	4.41	1.41		8.12	4.40	1.47		8.18	4.25	1.36		7.91	4.32	1.41	
^{150}Thr/Ahx	8.11	4.29	4.24	1.20	7.87	4.33	nd	1.23	7.84	3.15	1.63	1.30 1.50 2.33	7.66	3.22	1.65	1.35 1.54 2.35
^{151}–/Cys	-	-	-	-	-	-	-	-	8.44	4.68	3.30 3.00		8.25	4.76	3.32 3.04	

ne, non existing; nd, not determined.

Conformational chemical shifts

The first structural information derived from the NMR experiments was based on the conformational chemical shifts plotted in Fig. 2.21. As can be seen, neither peptide shows any marked tendency to adopt a predominant canonical (helix or β-sheet) conformation in solution. The small absolute values of the conformational chemical shifts suggest that both peptides exist mainly in aperiodic (random coil) form in solution. This lack of structuration could not be modified by environmental changes, as shown by the similarity between conformational chemical shifts observed in water and in 30% TFE.

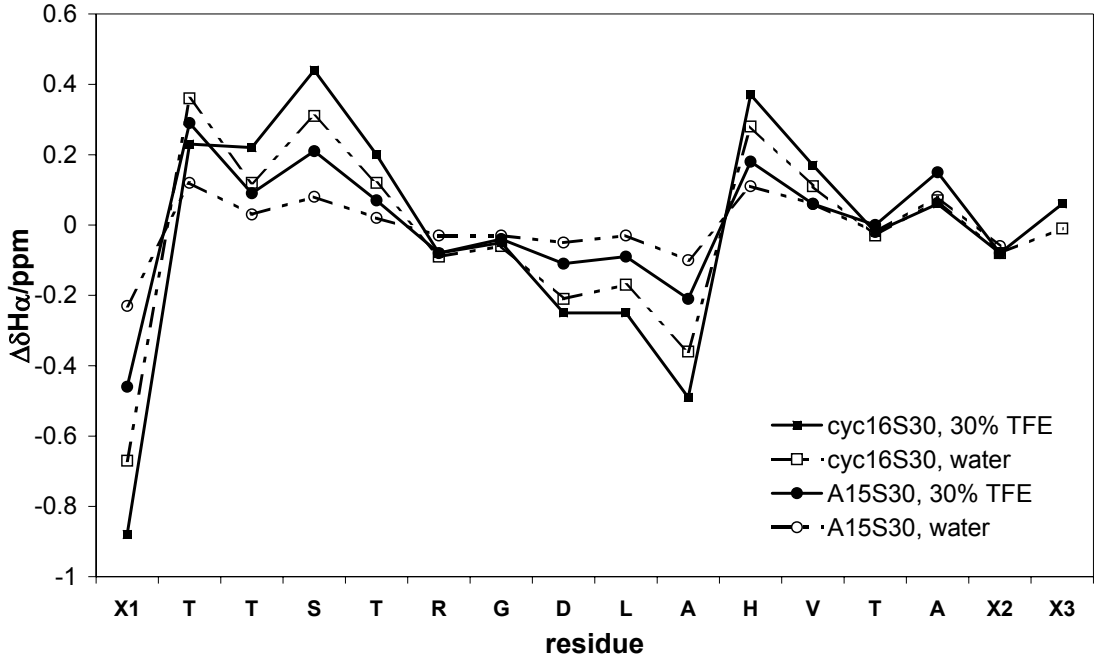

Figure 2. 21 Conformational chemical shifts ($\Delta\delta H^{\alpha}$) observed at 25 ºC for peptides A15S30 (Xaa=Tyr, Yaa=Thr, Zaa= -) and cyc16S30 (Xaa=Cys, Yaa=Ahx, Zaa=Cys) both in water and in 30% TFE.

Nevertheless, a slight tendency to structuration in the central region of the peptides can be distinguished. As previously observed by T. Haack and co-workers for the linear (A15) and cyclic disulphide (AhxA16SS) versions of FMDV C-S8c1[19,30], the conformational chemical shifts in the region that includes the RGD tripeptide are compatible with a tendency for an open turn conformation. Further, the cluster of negative conformational chemical shifts from ^{143}Asp to ^{146}His could be suggestive of an incipient short helix in this region, as previously observed for the C-S8c1 peptides by the same authors. A significant difference between the peptides of both strains is, however, the fact that this short helix extends, in the C-S8c1 peptides, to the ^{147}Leu residue. In the case of the C-S30 peptides, the replacement of leucine by valine at this position seems to shorten this pre-helical stretch, and this could be related to the lower antigenicities observed in peptides including this replacement. This seems further supported by the fact that absolute values of conformational chemical shifts in this region are higher for cyclic peptide cyc16S30, which is the best of the two C-S30 antigens under study.

Structural information from NOEs

Data from NOE experiments were not particularly conclusive. A continuous series of $\alpha N_{i,i+1}$ and $\beta N_{i,i+1}$ NOEs was observed for both peptides either in water or in 30% TFE (Fig. 2.22). These NOEs are compatible with practically all conformations and therefore not very informative. Some weak $NN_{i,i+1}$ NOEs – compatible with α helix – were observed for peptide A15S30 in 30% TFE, in the same region where a tentative assignment of incipient helix had been made (see previous section). In turn, peptide cyc16S30 displayed weak $NN_{i,i+1}$ NOEs both in water and 30% TFE (Fig. 2.23). Peak assignment was often ambiguous due to identical chemical shifts for different H^N and peak overlap possibly prevented the detection of other informative H^N – H^N connectivities.

Figure 2. 22 Summary of the NOEs observed for peptides A15S30 and cyc16S30 in water and 30% TFE; relative NOE intensities are represented by bar thickness; dotted lines stand for overlapping or ambiguous NOEs.

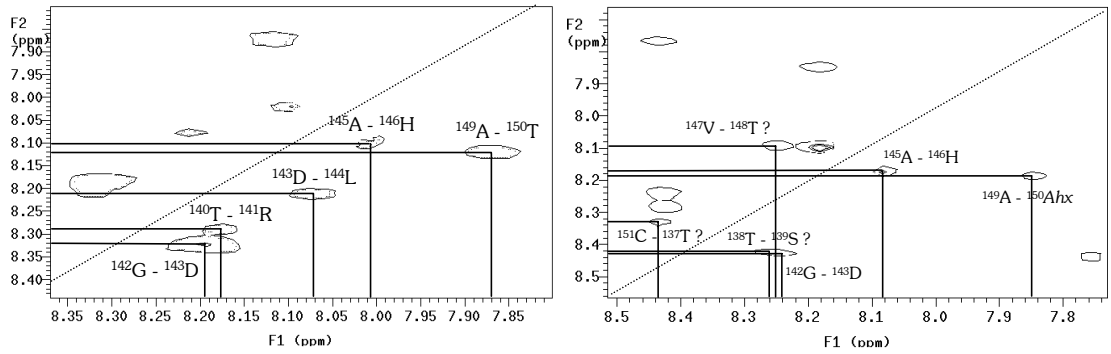

Figure 2. 23 Expansion of the ROESY experiments (200 ms) performed at 25 °C: peptide A15S30 in 30% TFE (left) and peptide cyc16S30 in water (right). Diagonal peaks (along the dashed lines) were omitted for simplicity.

2.9 Recapitulation

The work described in the present chapter involved a major goal:

Finding out why FMDV C-S30 was recognised and neutralised by anti-site A antibodies such as 4C4, even though it possesses, within this site, mutations known to be detrimental for mAb recognition (e.g., $^{147}L \rightarrow V$).

To accomplish such purpose, a total of sixteen peptides were synthesised and studied by SPR. ELISA and NMR analyses were also performed on some of these peptides, to further complement the study of the GH loop from FMDV C-S30. Extensive research previously reported on 15-mer peptide mimics of FMDV antigenic site A provided a solid basis for the adequacy of such peptides as models of this antigenic site.

The first set of eleven peptides corresponded to linear pentadecapeptides reproducing all possible combinations of the four mutations ($^{138}A \rightarrow T$, $^{140}A \rightarrow T$, $^{147}L \rightarrow V$, $^{149}T \rightarrow A$) present in FMDV C-S30 antigenic site A (taking as reference sequence the antigenic site A of FMDV C- S8c1).
A direct kinetic SPR analysis of the mAb – peptide interactions was performed according to a protocol previously optimised and validated with similar peptide FMDV antigens (chapter 1). Results pointed to additive effects in all combinations of the four relevant mutations. For each mAb, association rate constants were virtually equal, while dissociation rate constants varied in a relatively broad range, increasing with decreasing peptide antigenicity.
The four-point mutant linear 15-mer peptide from the C-S30 GH loop (A15S30) was shown to be the least antigenic of the set.

The surprisingly low antigenicity of peptide A15S30 led to a competition ELISA screening of all 15-mer peptides, in order to confirm the SPR data.
Peptide A15S30 was again shown to be a poor competitor in this format of analysis, thus confirming its low antigenicity relative to C-S8c1 or C_1-Brescia peptides.

Having confirmed that the unexpected results obtained for A15S30 were not due to any technical artefact from the SPR biosensor, our attention was then focused on the peptide itself: *was the peptide too short?*
Two 21-mer linear peptide models of the C-S8c1 and C-S30 GH loops were then studied by kinetic SPR analysis and competition ELISA.
Peptide C-S30 was, once again, clearly less antigenic than peptide C-S8c1.

At this point of the investigation, parallel studies performed by Wendy F. Ochoa and co-workers showed that the 15-mer peptide A15S30 could be crystallised in complex with the Fab fragment of mAb 4C4. The peptide adopted a nearly cyclic conformation similar to the one previously described for the C-S8c1 peptide A15 in a similar complex. Further, it was observed that the two more critical mutations (^{138}A→T and ^{147}L→V), although not in direct interaction with the antibody, were both involved in keeping the peptide in a pseudo-cyclic conformation, through hydrogen bonding involving the Thr side chain hydroxyl, one water molecule and the main chain oxygen atoms of ^{144}Leu and ^{147}Val.

So, a new question was immediately raised: *Were the linear C-S30 peptides too flexible in solution*?

Two cyclic disulphide peptides were thus studied by SPR, one of them reproducing the C-S30 sequence (cyc16S30) and the other containing the one-point mutation ^{147}L→V (cyc16^{147}Val) in order to analyse the effects of conformation modulation on peptide antigenicity.

An increase in peptide affinity was observed upon cyclization. While the single-point was still more antigenic than the four-point mutant towards mAb SD6, a reversion in this ranking was observed with mAb 4C4.

The higher antigenicity of C-S30 cyclic peptides and the results obtained by Wendy F. Ochoa with the linear C-S30 peptide led to another question: *Would the flexible peptide A15S30 be able to rearrange in order to form a stable* complex *with anti-site A mAb 4C4 in solution, after prolonged incubation?*

To answer this question, a solution affinity SPR experiment was performed using peptides A15(147V), A15S30, cyc16S30 and cyc16^{147}Val as target analytes and peptides A15 and A15Brescia as reference analytes. ***Despite confirming that linear C-S30 peptides were again less antigenic than their C-S8c1 or C_1-Brescia counterparts after overnight incubation with mAb in solution, a significant increase (about one order of magnitude) in 4C4 affinity towards peptide A15S30 was observed. This suggests that, indeed, incubation of 4C4 with A15S30 can lead the peptide to rearrange and form a stable complex with antibody.***

Solution conformation NMR studies of both A15S30 and cyc16S30 peptides, though not totally conclusive, were quite suggestive. ***Both peptides were seen to be very flexible in solution, even in the presence of conformation-inducing solvents. Nevertheless, both displayed a tendency for an open turn in the RGD region, followed by an incipient short helical path, as previously observed for C-S8c1 linear and cyclic peptides. Remarkably, while in the C-S8c1 peptides this helical stretch extends up to the ^{147}Leu, in the C-S30 peptides it stops at the ^{146}His, suggesting that a ^{147}Leu→Val helix-disruptive mutation could be the basis for the lower antigenicites observed in peptides including this mutation. Further, this short helix is more pronounced in the cyclic model of the C-S30 GH loop, which can be a reason for the higher antigenicities observed for this peptide.***

References

1 Mateu, M. G., Rocha, E., Vicente, O., Vayreda, F., Navalpotro, C., Andreu, D., Pedroso, E., Giralt, E., Enjuanes, L. and Domingo, E. (1987) Reactivity with monoclonal antibodies of viruses from an episode of foot-and-mouth disease, *Virus Res.* ***8***, 261-274.

2 Mateu, M. G., da Silva, J. L., Rocha, E., de Brum, D. L., Alonso, A., Enjuanes, L., Domingo, E. and Barahona, H. (1988) Extensive antigenic heterogeneity of foot-and-mouth disease virus serotype C, *Virology* ***167***, 113-124.

3 Mateu, M. G., Martínez, M. A., Andreu, D., Parejo, J., Giralt, E., Sobrino, F. and Domingo, E. (1989) Implications of a quasispecies genome structure: effect of frequent, naturally occurring, amino acid substitutions on the antigenicity of foot-and-mouth disease virus, *Proc. Natl. Acad. Sci. USA* ***86***, 5883-5887.

4 Mateu, M. G., Martínez, M. A., Cappucci, L., Andreu, D., Giralt, E., Sobrino, F., Brocchi, E. and Domingo, E. (1990) A single amino acid substitution affects multiple overlapping epitopes in the major antigenic site of foot-and-mouth disease virus of serotype C, *J. Gen. Virol.* ***71***, 629-637.

5 Martínez, M. A., Hernández, J., Piccone, M. E., Palma, E. L., Domingo, E., Knowles, N. and Mateu, M. G. (1991) Two mechanisms of antigenic diversification of foot-and-mouth disease virus, *Virology* ***184***, 695-706.

6 Mateu, M. G., Andreu, D., Carreño, C., Roig, X., Cairó, J. J., Camarero, J. A., Giralt, E. and Domingo, E. (1992) Non-additive effects of multiple amino acid substitutions on antigen-antibody recognition, *Eur. J. Immunol.* ***22***, 1385-1389.

7 Carreño, C., Roig, X., Camarero, J. A., Cairó, J. J., Mateu, M. G., Domingo, E., Giralt, E. and Andreu, D. (1992) Studies on antigenic variability of C-strains of foot-and-mouth disease virus by means of synthetic peptides and monoclonal antibodies, *Int. J. Peptide Protein Res.* ***39***, 41-47.

8 Fields, G. B. and Noble, R. L. (1990) Solid-phase peptide synthesis utilizing 9-fluorenylmethoxycarbonyl amino acids, *Int. J. Peptide Protein Res.* ***53***, 161-214.

9 Knorr, R., Trzeciak, A., Bannwarth, W. and Gillesen, D. (1989) New coupling reagents in peptide chemistry, *Tetrahedron Lett.* ***30***, 1927-1930.

10 Bernatowicz, M. C., Daniels, S. B. and Köster, H. (1989) A comparison of acid labile linkage agents for the synthesis of peptide C-terminal amides, *Tetrahedron Lett.* ***30***, 4645-4648.

11 O'Shannessy, D. J. and Winzor, D. J. (1996) Interpretation of deviations from pseudo-first-order kinetic behavior in the characterization of ligand binding by biosensor technology, *Anal. Biochem.* ***236***, 275-283.

12 Schuck, P. (1997) Reliable determination of binding affinity and kinetics using surface plasmon resonance biosensors, *Curr. Op. Biotech.* ***8***, 498-502.

13 Hall, D. R., Cann, J. R. and Winzor, D. J. (1996) Demonstration of an upper limit to the range of association rate constants amenable to study by biosensor technology based on surface plasmon resonance, *Anal. Biochem.* ***235***, 175-184.

14 Verdaguer, N., Sevilla, N., Valero, M. L., Stuart, D., Brocchi, E., Andreu, D., Giralt, E., Domingo, E., Mateu, M. G. and Fita, I. (1998) A similar pattern of interaction for different antibodies with a major antigenic site of foot-and-mouth disease virus: implications for intratypic antigenic variation, *J. Virol.* ***72***, 739-748.

15 Mateu, M. G., *personal communication*

16 Abbas, A. K., Lichtman, A. H. and Pober, J. S. "Cellular and molecular immunology", 3rd ed., W. B. Saunders Co., United States of America (1997).

17 Mateu, M. G., Andreu, D. and Domingo, E. (1995) Antibodies raised in a natural host and monoclonal antibodies recognize similar antigenic features of foot-and-mouth disease virus, *Virology* ***210***, 120-127.

18 Ochoa, W. F., Kalko, S., Mateu, M., Gomes, P., Andreu, D., Domingo, E., Fita, I. and Verdaguer, N. (2000) A multiply substituted GH loop from foot-and-mouth disease virus in complex with a neutralizing antibody: a role for water molecules, *J. Gen. Virol.* ***81***, 1495-1505.

19 Valero, M. L., Camarero, J. A., Haack, T., Mateu, M. G., Domingo, E., Giralt, E. and Andreu, D. (2000) Native-like cyclic peptide models of a viral antigenic site: finding a balance between rigidity and flexibility, *J. Mol. Recognit.* ***13***, 5-13.

20 Andreu, D., Albericio, F., Solé, N. A., Munson, M. C., Ferrer, M. and Barany, G. Formation of disulfide bonds in synthetic peptides and proteins in "Methods in molecular biology, vol. 35: Peptide synthesis protocols", Pennington, M. W. and Dunn, B. M. (Eds.), Humana Press Inc., Totowa, New Jersey (1994), pp 91-169.

21 Ellman, G. L. (1958) A colorimetric method for determining low concentrations of mercaptans, *Arch. Biochem. Biophys.* ***74***, 443-450.

22 "BIAapplications Handbook", (Pharmacia Biosensor AB, 1994) Uppsala, Sweden.

23 Nieba, L., Krebber, A. and Plükthun, A. (1996) Competition BIAcore for measuring true affinities: large differences from values determined from binding kinetics, *Anal. Biochem.* ***234***, 155-165.

24 "BIAevaluation Software Handbook: version 3.0", (Biosensor AB, 1997) Uppsala, Sweden.

25 Lazareno, S. and Birdsall, N. J. (1993) Estimation of competitive antagonist affinity from functional inhibition curves using the Gaddum, Schild and Cheng-Prusoff equations, *British J. Pharmacol.* ***109***, 1110-1119.

26 Wüthrich, K. "NMR of proteins and nucleic acids", Wiley, New York (1986).

27 Braunschweiler, L. and Ernst, R. R. (1983), *J. Magn. Reson.* ***53***, 521.

28 Kumar, A., Ernst, R. R. and Wüthrich, K. (1980), *Biochem. Biophys. Chem. Comm.* ***95***, 1.

29 Bothner-By, A. A., Stephens, R. L., Lee, J., Warren, C. D. and Jeanloz, R. W. (1984) Structure determination of a tetrasaccharide: transient nuclear overhauser effects in the rotating frame, *J. Am. Chem. Soc.* ***106***, 811-813.

30 Haack, T., Camarero, J. A., Roig, X., Mateu, M. G., Domingo, E., Andreu, D. and Giralt, E. (1997) A cyclic disulfide peptide reproduces in solution the main structural features of a native antigenic site of foot-and-mouth disease virus, *Int. J. Biol. Macromol.* ***20***, 209-219.